

Chapter 4

Transient Photoconductivity Decay Measurements of Polymer-Terminated Silicon Surfaces

1. Introduction

The fabrication of conducting and/or nonconducting organic overlayers on crystalline Si surfaces is of interest for inhibiting of surface corrosion processes,¹ for providing routes to chemical control over the electrical properties of Schottky barrier-like structures,² for enabling novel lithographic strategies that utilize contact printing and photopatterning,³⁻⁵ for producing novel metal-insulator-semiconductor devices,⁶ and for controlling the electrical recombination properties of Si surfaces,^{7,8} amongst other applications. To obtain acceptable electrical device properties, many of these applications require direct functionalization of the Si surface in a fashion that does not introduce significant densities of interfacial electronic defect levels. The presence of a native oxide on Si is largely unacceptable for such purposes because the resulting Si/Si oxide interface is often highly electrically defective.^{9,10} In addition, the oxide acts as a tunneling barrier for charge carriers and the uniformity of this barrier is difficult to control at the molecular level. Thermally grown silicon oxides generally contain fixed positive charge,^{9,11-13} which also limits the types of electrical device behavior that can be obtained from such interfaces. The ability to form electrically conductive or nonconductive overlayers of controlled thickness on Si without relying on reactions that utilize functionality arising from native and/or thermally grown Si oxides would be important and desirable for future technological advancements.

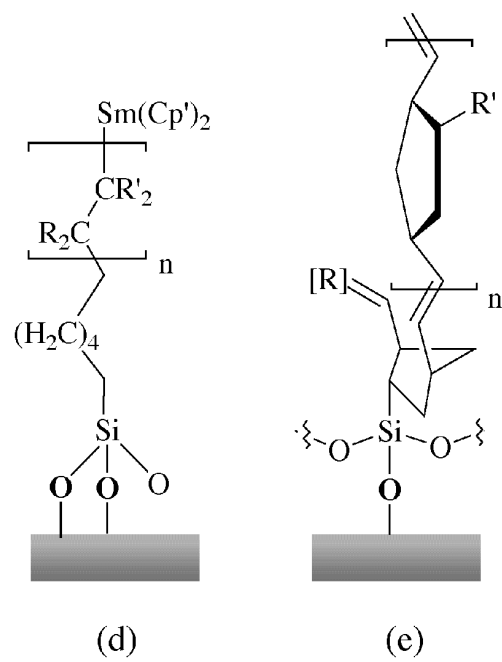
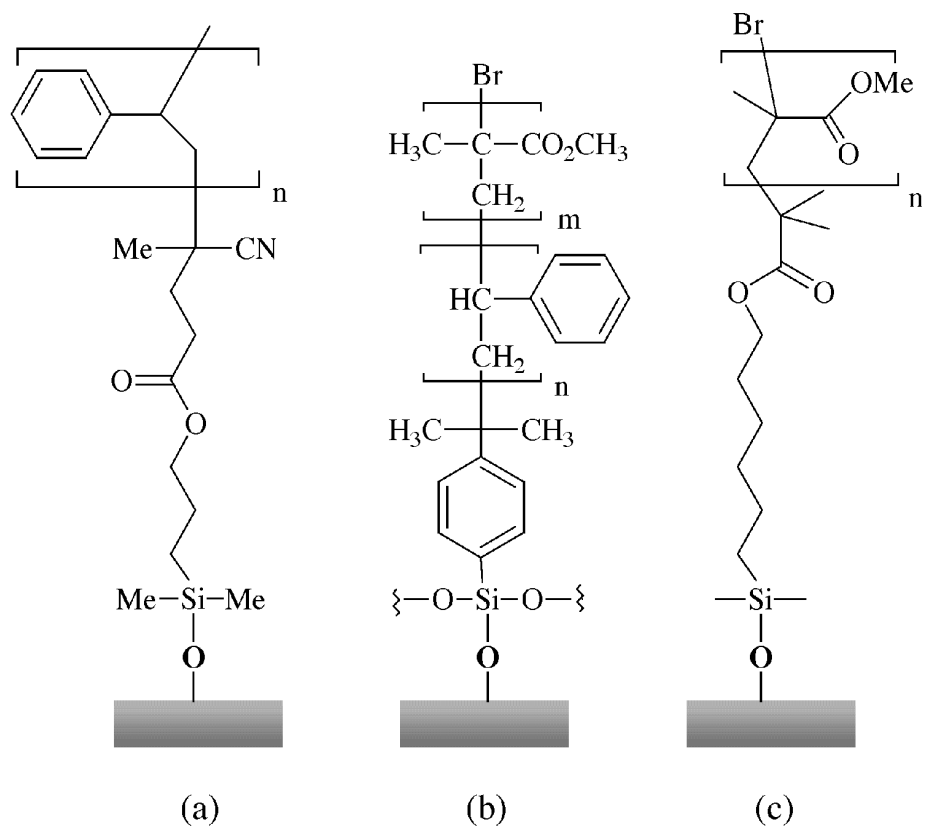
Langmuir-Blodgett techniques¹⁴ have been used to synthesize organic thin films with controlled structure and composition; however, the fragility of the resulting films represents a major obstacle to practical implementation. Another method that has been adopted for controlling the surface properties of a solid is by functionalizing the surface with tethered polymer chains, called polymer brushes. Polymer brushes are polymers confined to a small volume near an interface, and restrictions due to steric requirement

force the chains to stretch away from the grafting point to the edge of polymer layer. Several strategies have been employed to prepare brush-type polymer layers, including selective physisorption of block copolymers,¹⁵⁻¹⁷ chemical grafting of preformed polymer chains onto the surface (“grafting to”),¹⁸⁻²⁰ and “grafting from” methods that involve surface-initiated polymerization.²¹⁻²⁷ As adsorbed block copolymers face a disadvantage of thermal instability, more robust films have been obtained using polymers with functionalities appropriate for covalent attachment to surfaces. The significant improvement in physical properties, however, generally is accompanied by a loss of control over the order and composition of the overlayer. The “grafting to” approach also produces polymer layers with low grafting density. Crowding of the chains at the surface occurs as more polymers are grafted onto the substrate, which hinders the diffusion of reactive chain ends to the surface for further grafting. The surface-initiated polymerization can overcome this limitation by first attaching reactive units that are able to initiate polymerization on the substrate, leaving the propagating polymer chains to grow away from the surface. Since the smaller monomer can readily access the initiator site at the end of propagating chain, the grafting density is greatly increased. Examples of the “grafting from” method for Si surface modification include radical chain polymerization initiated by surface-bound azo compounds,²⁴ sequential cationic and atom transfer radical polymerization,²⁵ living free radical polymerization,²⁷ polymerization by organometallic initiators,²⁶ and ring-opening metathesis polymerization.²¹ However, all these polymerization techniques utilize the reactions between chlorosilane moieties and silicon oxide surfaces, and result in an intervening Si oxide layer between the Si and surface functionality (see Figure 4.1). In order to prepare polymer-modified Si surfaces that are suitable for electronic device applications, a method was developed for the formation of an organic overlayer directly on the Si substrate through a covalent Si-C linkage.

Crystalline Si has recently been functionalized using a variety of approaches;²⁸⁻⁴² notably, alkylation of crystalline, (111)-oriented Si using a two-step chlorination/alkylation procedure can produce functionalized surfaces that have a very low surface recombination velocity.^{8,43} This modification method was developed and thoroughly characterized by Ashish Bansal, and was crucial for the work of this chapter. The work described in this chapter was also inspired in part by a prior study of Weck et al., who first showed the possibility of producing surface-immobilized polymer brushes using surface-initiated ring-opening metathesis polymerization (ROMP). They reported the polymerization of substituted norbornenes from a modified gold surface using a Ru-based alkylidene as initiator, though only small amounts of polymer chains were formed.⁴⁴ This chapter describes the extension of chlorination/alkylation chemistry, combined with ROMP methods, to produce polymer overlayers that are covalently attached directly to a Si(111) surface and provide molecular-level control over the thickness and electronic properties of the resulting Si/polymer contacts.

Figure 4.1

Examples of polymer-terminated Si reported in literature utilizing “graft from” approach to form covalently attached polymers or block copolymers on Si surfaces. The surface-initiated polymerization method includes (a) radical chain polymerization initiated by surface-bound azo compounds,²⁴ (b) sequential cationic and atom transfer radical polymerization,²⁵ (c) living free radical polymerization,²⁷ (d) polymerization by organometallic initiators,²⁶ and (e) ring-opening metathesis polymerization.²¹ All above methods relied on chlorosilane chemistry to link the polymer layer to the SiO₂ substrate, and resulted in an intervening oxide layer which can be unsuitable for electronic device applications that require a low surface defect density.



2. Experimental

2.1. Chemicals

All solvents used for surface modification, including acetonitrile, chlorobenzene, 1,2-dichloroethane, dichloromethane, methanol, and tetrahydrofuran (THF), were purchased from Aldrich or Acro in the anhydrous form and used as received. Solvents were stored over activated 3 Å molecular sieves (EM Science) in an N₂(g)-purged glove box. Solvents used for wafer degreasing, acetone, dichloromethane, methanol, and 1,1,1-trichloroethane, were either reagent grade (GR) or Omnisolve grade obtained from EM Science and used as received. Hydrogen peroxide (30%) was purchased from EM Science, and H₂SO₄(aq) was obtained from J.T. Baker. Hydrofluoric acid buffered with ammonium fluoride (NH₄F/HF, buffered HF) and 40% ammonium fluoride (NH₄F) solutions were purchased from Transene Co. Phosphorus pentachloride (PCl₅), benzoyl peroxide, allylmagnesium chloride (CH₂=CHCH₂MgCl, 1.0 M in THF) were obtained from Aldrich and were used without further purification. The ring-opening metathesis catalyst [RuCl₂(=CHPh)(PCy₃)₂, Cy = cyclohexyl] (**1**) was obtained from Materia while [RuCl₂(=CHPh)(PCy₃)(IMesH₂), IMes = dimesityl-imidazolidene] (**2**) was provided by O. A. Scherman.⁴⁵ Monomers norbornene (Aldrich) and dicyclopentadiene (DCPD, Materia) were dissolved in anhydrous 1,2-dichloroethane and anhydrous dichloromethane, respectively. 1,3,5,7-Cyclooctatetraene (COT) was obtained from BASF and dried over CaH₂, while 1,5-Cyclooctadiene (COD) was purchased from Aldrich. Both COD and COT were distilled before used. C5, C4, and C6 olefin Grignard reagents, 4-pentenylmagnesiumbromide (CH₂=CH(CH₂)₃MgBr, ~1.0 M in THF), 3-butenylmagnesiumbromide (CH₂=CH(CH₂)₂MgBr, ~1.5 M in THF) and the 5-

hexenylmagnesiumbromide ($\text{CH}_2=\text{CH}(\text{CH}_2)_4\text{MgBr}$, ~ 1.0 M in THF), were provided by O. A. Scherman.

2.2. Preparation of Substrates

Single-crystal, (111)-oriented, *n*-type float-zone silicon wafers were obtained from Topsil Semiconductor Materials. The double-side polished wafers were 280 ± 20 μm thick, and phosphorous-doped with resistivities of 3500–6500 $\Omega\cdot\text{cm}$ as specified by the manufacturer. The bulk lifetime of 6760 μs was measured by the photoconductive decay method at the manufacture. The silicon wafers were first oxidized in a “Pirhana” solution which consisted of 3:1 (v/v) concentrated $\text{H}_2\text{SO}_4(\text{aq})$: H_2O_2 (30%) heated to approximately 100 $^\circ\text{C}$ for one hour.³³ **Caution:** *The acidic “Pirhana” solution is extremely dangerous, particularly in contact with organic materials and should be handled carefully.* The wafers were then rinsed with copious amount of 18.0 $\text{M}\Omega\cdot\text{cm}$ resistivity water (obtained from a Barnstead Inc. Nanopure water purification system), dried under pressurized $\text{N}_2(\text{g})$, and stored for future use. Before surface modifications, the wafer was cut into approximately 9 mm \times 9 mm size samples. Each piece was briefly sonicated in 18.0 $\text{M}\Omega\cdot\text{cm}$ resistivity water, degreased by rinsing sequentially with methanol, acetone, 1,1,1-trichloroethane, dichloromethane, 1,1,1-trichloroethane, acetone, and methanol, and followed by another brief sonication in water. After blow drying with $\text{N}_2(\text{g})$, the samples were etched in $\text{NH}_4\text{F}/\text{HF}$ (buffered HF) for 30 seconds, and then directly immersed in 40% NH_4F for 15–20 min.⁴⁶ Following the etching process, the samples were rinsed with 18.0 $\text{M}\Omega\cdot\text{cm}$ resistive water (obtained from Barnstead E-pure filtration system), and dried under a stream of $\text{N}_2(\text{g})$. The samples were quickly mounted onto the XPS stubs and introduced into ultrahigh vacuum (UHV) system that houses the x-ray photoelectron spectroscopy (XPS) via an atmospheric load lock for immediate surface characterization.

2.3. Surface Modification

All surface modification procedures were carried out in an N₂(g)-purged glove box which is connected to the UHV system housing the XPS spectrometer via a gate valve. Figure 4.2 depicts the schematic experimental approach: (i) an alkenyl linker of variable length is coupled to a chlorinated Si surface using a Grignard reaction; (ii) an olefin cross-metathesis reaction is used to obtain a surface-bound ruthenium ring-opening metathesis polymerization (ROMP) catalyst layer, and (iii) a monomer is added to effect growth of polymer onto the surface.

2.3.1. Chlorination

After verifying that the etching process was successful as determined by the absence of oxide on the Si surfaces, the samples were brought into the N₂(g)-purged glove box directly through the gate valve. The stock chlorinating solution was prepared by dissolving excess PCl₅ in chlorobenzene to form a saturated solution (typically 0.6–0.7 M). The solution was warmed to about 60 °C for at least 1 hour to dissolve as much PCl₅ as possible. Immediately before use, a small portion of the stock chlorinating solution was poured into a small beaker, and a few grains of benzoyl peroxide were added (approximately 30–40 mg of benzoyl peroxide in 10 ml of PCl₅-chlorobenzene solution) as a radical initiator.^{47,48} With the samples completely immersed in this solution and the beaker covered by a watch glass, the reaction was heated to 90–100 °C for 45–60 min. The samples were then taken out of the chlorinating solution, rinsed with anhydrous THF followed by anhydrous methanol or anhydrous dichloromethane, and dried in a stream of N₂(g). Some samples were mounted on the XPS stub and brought into the UHV system for surface characterization.

2.3.2. Terminal-Olefin Addition via Grignard Reaction

The chlorinated Si samples were placed in separate test tubes so that Si pieces were in standing position and the surfaces did not touch the bottom of reaction vessels. The olefin Grignard reagent was then added to each test tube and heated to 65–80 °C for 8–18 hours. The reaction time varied according to the chain length of the terminal olefin group (see Table 4.1). Two procedures requiring different types of test tubes and rinsing solvents were adapted depending on the Grignard reagent used. When allylmagnesium chloride (Aldrich) or C4 olefin Grignard was used, the reaction took place in test tubes capped with septa. Following the overnight reaction, the samples were rinsed with copious amount of anhydrous THF and anhydrous methanol, individually immersed in anhydrous methanol in screw-capped vials, and taken out of the glove box for sonication. The derivatized samples were sonicated in anhydrous methanol and anhydrous acetonitrile for 5 min each, dried in a stream of N₂(g) before being mounted on the XPS stub, and introduced into UHV through atmospheric load lock for surface characterization.

Due to a longer reaction time when C5 or C6 olefin Grignard was used, it was necessary to eliminate as much methanol vapor in the glove box as possible. Prior to the reaction, fresh phosphorous pentoxide (P₂O₅) powders were poured into an evaporation dish and used as a drying agent to absorb solvent vapors in the glove box. Anhydrous dichloromethane was used in place of anhydrous methanol throughout the surface modification procedures. The samples were immersed in anhydrous dichloromethane when taken out of the glove box and sonicated in anhydrous dichloromethane, anhydrous methanol, and anhydrous acetonitrile for 5 min each. During the reaction, the samples were also isolated from the glove box atmosphere by using teflon-lined screw-capped test tubes instead of septa-capped ones. For each experiment, only a fresh portion of homemade Grignard reagent was brought into the glove box in a Schlenk tube, and the

portion was defrosted by warming to ~ 45 °C immediately before use. Allylmagnesium chloride bottle was stored in the glove box for no more than one month, and the solution was drawn with a syringe through the Sure/Seal cap.

2.3.3. Catalyst Addition

Olefin-terminated-Si samples were placed into several screw-capped vials containing a ruthenium-alkylidene ring-opening metathesis catalyst solution for at least 3 hours. Then the samples were washed copiously with anhydrous dichloromethane and dried with a stream of $N_2(g)$. The ruthenium catalyst solution was made immediately prior to use by dissolving $Cl_2(Cy_3P)_2Ru=CHPh$ (**1**, ~ 25 mM) in anhydrous dichloromethane. A more powerful catalyst $Cl_2(H_2IMes)(PCy_3)Ru=CHPh$ (**2**, ~ 10 mM in anhydrous dichloromethane) was also used for some experiments involving polymerizing cyclooctatetraene (COT) and norbornene.

2.3.4. Polymerization

The stock norbornene solution (2.44 M) was made by dissolving norbornene in anhydrous 1,2-dichloroethane and stored in a Schlenk tube covered with an aluminum foil. In screw-capped vials, less concentrated norbornene solutions (0.01 M, 0.05 M, 0.09 M, 0.15 M, 0.18 M, 0.27 M, and 0.45 M) were made from the stock prior to catalyst addition reaction. This is to minimize the exposure of the stock solution to any ruthenium catalyst in the glove box atmosphere. Small vials that allow only the edges of a sample to touch the vial wall and the bottom were used. The desired monomer solution was then added into the vials and the vials were capped quickly. The standard reaction time for norbornene, COD, and COT was 30 min at room temperature, and then washed with copious amount of anhydrous dichloromethane and dried in a stream of $N_2(g)$. The dicyclopentadiene (DCPD) polymerization was carried out by first immersing the samples in a DCPD solution (2.5 M in dichloromethane) for 30 min at room temperature.

Then the DCPD solution was drained, and the vials and samples were washed with anhydrous dichloromethane. A fresh portion of anhydrous dichloromethane was added into the vials, and the samples were then heated to $\sim 40\text{--}50\text{ }^{\circ}\text{C}$ for 5–10 min to allow cross-linking of attached polymer. Samples were washed and dried the same way.

At least one sample per batch was characterized by XPS, and these samples were not used in the photoconductivity decay measurements. The XPS samples were mounted onto the stub and transferred into the glove box load lock through the gate valve, while samples for the photoconductivity decay measurements were placed separately in the open glass vessels and pumped in the antichamber of the glove box for at least 3 hours. Before performing the photoconductivity decay measurements, samples were taken into the glove box and sealed in glass vessels under $\text{N}_2(\text{g})$, and then brought out of the glove box for measurements. For overlayer thickness measurements and scanning electron microscopy, samples were mounted onto the XPS stub, characterized by XPS, and then taken out through the atmospheric load lock.

2.4. Surface Characterizations

2.4.1. X-ray Photoelectron Spectroscopy

The XPS experiments were conducted in an M-probe surface spectrometer (VG Instrument) pumped by a CTI Cryogenics-8 cryo pump. Samples could be introduced into the UHV system using either the atmospheric load lock or the glove box load lock. The atmospheric load lock was pumped by a Varian model V80 turbo pump and a Varian model SD-300 mechanical pump, and allowed samples to be introduced into the UHV from air. The glove box load lock was pumped by a Varian model V200 turbo pump and a Varian model SD-300 mechanical pump, and enabled samples to be transferred into the UHV through a gate valve that opened to the $\text{N}_2(\text{g})$ -purged glove box. These load locks

were brought to the atmospheric pressure by back-filling with $N_2(g)$, and can be pumped down to approximately 10^{-7} Torr in about 10 min. Samples were mounted on a stainless steel or aluminum stub with screws.

The XPS chamber was maintained at a base pressure of less than 5×10^{-10} Torr, although the operating pressure was 5×10^{-9} to 2×10^{-8} Torr. Monochromatic Al K_{α} x-rays ($h\nu = 1486.6$ eV) incident at 35° from the sample surface were used to excite electrons from the sample, while the emitted electrons were collected by a hemispherical analyzer at a take-off angle of 35° from the plane of the sample surface. Data collection and analysis were done with the M-probe package software version 3.4. Survey scans were collected in the scanned mode with an elliptical spot of dimensions $800 \mu\text{m} \times 1200 \mu\text{m}$ incident on the sample surface. The high-resolution scans were recorded in an unscanned mode with the same spot size. A typical XPS characterization of a surface consisted of one survey scan from 0–700 eV binding energies and a high resolution scan of the Si 2p region (97.57–104.59 eV binding energies). In certain cases when Si 2p peak was very small or undetected, the high-resolution scan was omitted.

2.4.2. Overlayer Thickness Measurements: Ellipsometry and Profilometry

The thicknesses of polymer overlayers formed using different concentrations of norbornene and DCPD were measured by either ellipsometry or profilometry. Ellipsometric measurements were performed on a Gaertner variable angle ellipsometer model L116C using a helium-neon laser ($\lambda = 632.8$ nm) and a 45° polarizer, with an incident angle set to 70° . The film thickness was calculated using the software package provided by Gaertner. The index of refraction N_s and the absorption coefficient K_s of the substrate were determined using a freshly etched Si, and these numbers were used as standards when film thicknesses were measured. An index of refraction $N_F = 1.46$ was used for both terminal olefin and polymer layers. Film thickness was measured at six

different locations on each sample, and two measurements were done at each spot. The measured thickness values for all samples were $\pm 1 \text{ \AA}$ for a particular spot.

Profilometric measurements of several polynorbornene-terminated Si samples polymerized from 0.15M, 0.45 M, and 2.44 M norbornene solution were performed using Sloan Dektak 3030 surface profiling measuring system with a diamond stylus ($12.5 \mu\text{m}$ radius). The stylus force was set to 10 mN, and with the speed set to low, scan length of 4 mm was selected for most measurements. A stainless steel spatula was used to scrape away a thin stripe of the polynorbornene overlayer, and the profile of the surface features was plotted. By measuring the depth of the scribe, the thickness of the polymer was determined.

2.4.3. Scanning Electron Microscopy

Images of polynorbornene overlayers and sample cross section were obtained using Camscan series II scanning electron microscope (SEM). It was equipped with an Everhart-Thornley secondary-electron imaging, a Robinson-type backscattered electron detector for atomic-number-contrast imaging, and a relatively slow speed absorbed current imaging system. An on-board frame averaging system was used to integrate several scan frames in order to reduce noise, and the working resolution of the Camscan was approximately 100 nm. Digital imaging was performed using the 4Pi Systems Scanning Interface Unit for digital beam control, and images were acquired under an operating pressure of 10^{-5} Torr. The acquired digital images were stored in a computer and processed off-line using NIH Image program. Samples with different polynorbornene overlayer thicknesses were prepared using 0.15 M, 0.45 M, and 2.44 M norbornene solutions. The surface uniformity of the polymer layers was examined under a $500\times$ magnification. A cross-sectional SEM image of a sample prepared using 2.44 M norbornene/1,2-dichloroethane solution was also obtained under a $1500\times$ magnification and the polymer thickness was estimated from the image.

Figure 4.2

Experimental approach to produce a variety of covalently attached polymer overlayers on Si surfaces using surface-initiated ring-opening metathesis polymerization method. The structures of two metathesis catalysts used are shown in the box.

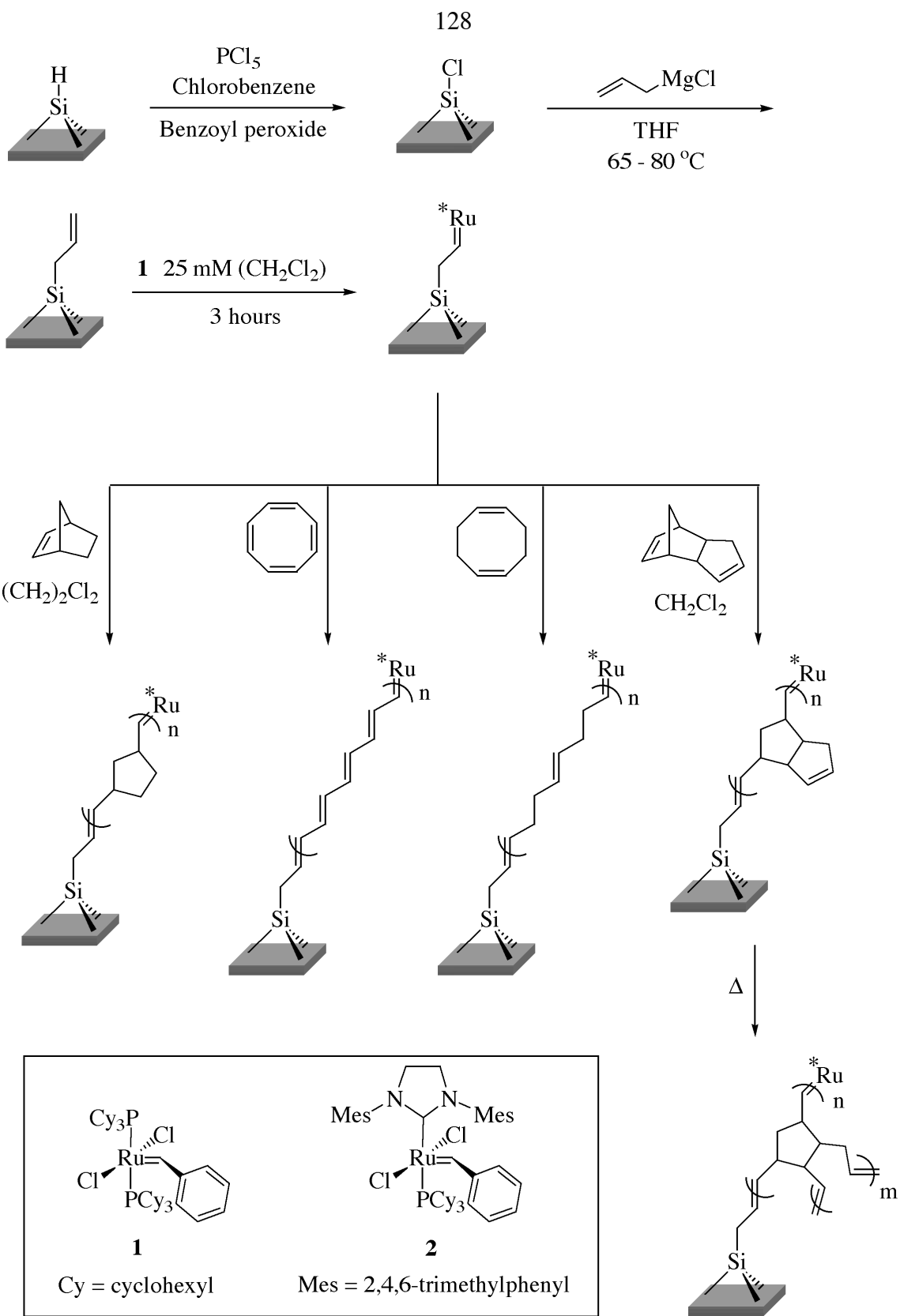
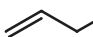

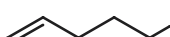
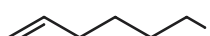


Table 4.1

List of reagents and reaction conditions used for each step of the Si surface modification procedure.

Reaction	Reagents	Reaction Time	Reaction Temperature
Chlorination	PCl ₅ in chlorobenzene + benzoyl peroxide	45 – 60 min	90 – 100 °C
Terminal Olefin Addition ^a	 MgCl	8 – 15 hr	65 – 80 °C
	 MgBr	8 – 15 hr	65 – 80 °C
	 MgBr	14 – 18 hr	65 – 80 °C
	 MgBr	16 – 18 hr	65 – 80 °C
Catalyst Addition ^b	Ru complex 1	3 hr	Room Temp.
	Ru complex 2	3 hr	Room Temp.
Polymerization	Norbornene in 1,2- dichloroethane	30 min	Room Temp.
	(1) DCPD in dichloromethane	30 min	Room Temp.
	(2) Heat treatment in dichloromethane	5 min	40 – 50 °C

^a The solvent used for this reaction was THF, and the approximate Grignard reagent concentrations were 1–1.5 M.

^b The solvent used to dissolve Ru complexes was anhydrous dichloromethane.

2.5. Photoconductivity Decay Measurements

A schematic of the contactless radio frequency (rf) conductivity apparatus used to measure photoconductivity decays is shown in Figure 4.3. In this system, the rf output from a high-frequency generator (Wavetek 2500A) operating at 450 MHz was connected to a power splitter (Mini-Circuits ZSC2-1W). One output from the power splitter was connected through an amplifier (ANZAC AM-147, +17 dB gain) and a phase-shifter (General Radio 847-LTL) to the local oscillator input of a double-balanced frequency mixer (Mini Circuits ZAY-2), and was used as a reference rf signal. The other output from the power splitter was connected through an amplifier (Mini-Circuits ZHL-1A, +20 dB gain) to the coupled port of a directional coupler (Merrimac CR-20-500, 20 dB isolation). An inductor-capacitor (LC) circuit consisting of a variable coupling capacitor (1-11 pF, air gap), a variable matching capacitor (1-11 pF, quartz), and a three-turn coil (Cu wire, 1.1 mm diameter) placed in close proximity to the sample, was connected to the input port of the directional coupler. The output port of the directional coupler was then connected through an attenuator (Kay 0/400A, 0 to -13 dB) to the reference oscillator port of the double-balanced frequency mixer. The output of the double-balanced frequency mixer was connected to a digital oscilloscope (Tektronix TDS-210) for the measurement of the photoconductivity decay signals.

Prior to a measurement, the LC circuit was tuned to the resonant frequency of the sample by adjusting the variable capacitors and monitoring the amplitude of the reflected rf signals on a separate high-frequency digital oscilloscope (Tektronix TDS-680c). A Spectra-Physics INDI-30 Nd:yttrium-aluminum-garnet laser (1064 nm) operating at a repetition rate of 10 Hz was used to illuminate samples with 10 ns pulses. The power density of the laser beam was attenuated using a beam splitter and neutral density filters (Hoya Optics), and the beam was expanded to approximately 2 cm² using a beam expander (Galilean). A spatially uniform beam profile was produced by placing a

holographic diffuser (Coherent, 1°) directly above the sample. The measurements were obtained under high-level injection conditions by adjusting the power density of the expanded incident beam to $\sim 1 \times 10^{-3}$ mJ pulse⁻¹ using neutral density filters. The incident beam power was determined using a power meter (Coherent Fieldmaster GS) equipped with a pyroelectric sensor (Coherent LM-P10i). The intensity of the light pulse at high-level injection was sufficient to eliminate equilibrium potential drop that might exist in the solid. Therefore imply that the changes in the observe carrier recombination lifetime are primarily due to changes in surface state density and/or the carrier-capture rate constants by surface traps. The sample was placed in a seal glass vessel which allows the sample to be in contact with either air or N₂(g) during the period of measurement. Time constants were obtained by fitting the average of 128 decays to a single exponential and averaging over a minimum of three samples for each type of surface and storage condition.

Time-resolved photoconductivity decays of six types of surfaces stored in a controlled environment at 21 °C and 7% relative humidity (R.H.) were recorded. In addition, three types of surfaces were subjected to a harsher environment at 40 °C and 80–90% R.H., and the effects on the photoconductivity decays were studied over a period of one month. The initial measurement for each type of surface was performed immediately after samples, sealed in the glass vessels under N₂(g), were taken out of the glove box. Then the glass vessels were opened to the air and the samples were stored under one of the two controlled environmental conditions.

The 21 °C/7% R.H. environmental chamber was made by feeding a constant flow of house air into a desiccator cabinet. An in-line oil-removal coalescing filter (Parker) in conjunction with a microalescer filter (Wilkerson) was used to remove oil droplets and vapor from the house air. Figure 4.4 displays the setup of the 40 °C/80–90% R.H. environmental chamber. The filtered house air was first split into two paths, and two Bel-Art Riteflow flowmeters were used to control the amount of air going through each

path. One path directed the air through a custom-made bubbler filled with deionized water (kept at ~ 45 °C) to allow saturation of water vapor, and then passed through a heat-exchange Cu coil immersed in a 45 °C constant-temperature bath/circulator (National Instrument Type SCI). The warmed water-vapor-saturated air was then combined with dry house air from the other path to create 80–90% R.H. and was introduced into a insulated chamber where the samples were stored. The warm water in the constant-temperature bath/circulator was also circulated through the outside jacket of the bubbler, and another heat-exchange Cu coil inside the insulated chamber designed to keep the air temperature at 40 °C. Samples were placed in separate test tubes while being stored in the 40 °C/80–90% R.H. chamber, and in plastic dishes if stored in the 21 °C/7% R.H. chamber. The relative humidity of each chamber was measured by a hygrometer (Control Company).

Figure 4.3

A schematic of the radio frequency (rf) apparatus used to perform photoconductivity decay measurements. The splitter separates the rf into reflected and reference signals. The imbalance in the circuit caused by the sample is phase detected by a double-balance frequency-mixer and then digitized. The attenuator in the reference branch of the circuit was bypassed in these experiments. The excess carriers generated by the light pulse injection cause an increase in electrical conductivity in the sample. The conductivity then decreases when these excess carriers recombine. The change in conductivity can be monitored by rf reflectance measurement, and the value of charge-carrier recombination lifetime can be obtained by analyzing the transient of the reflected rf power.

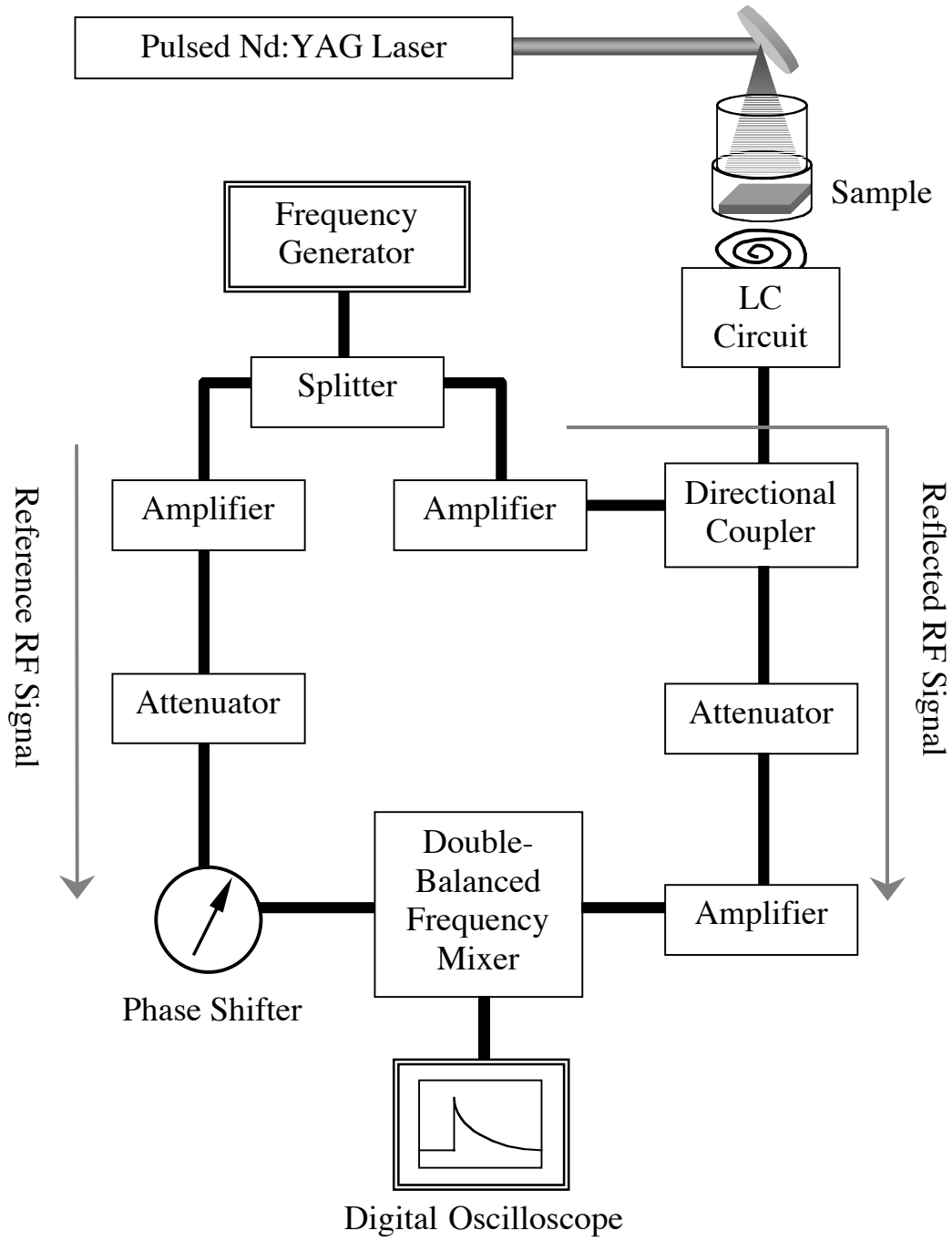
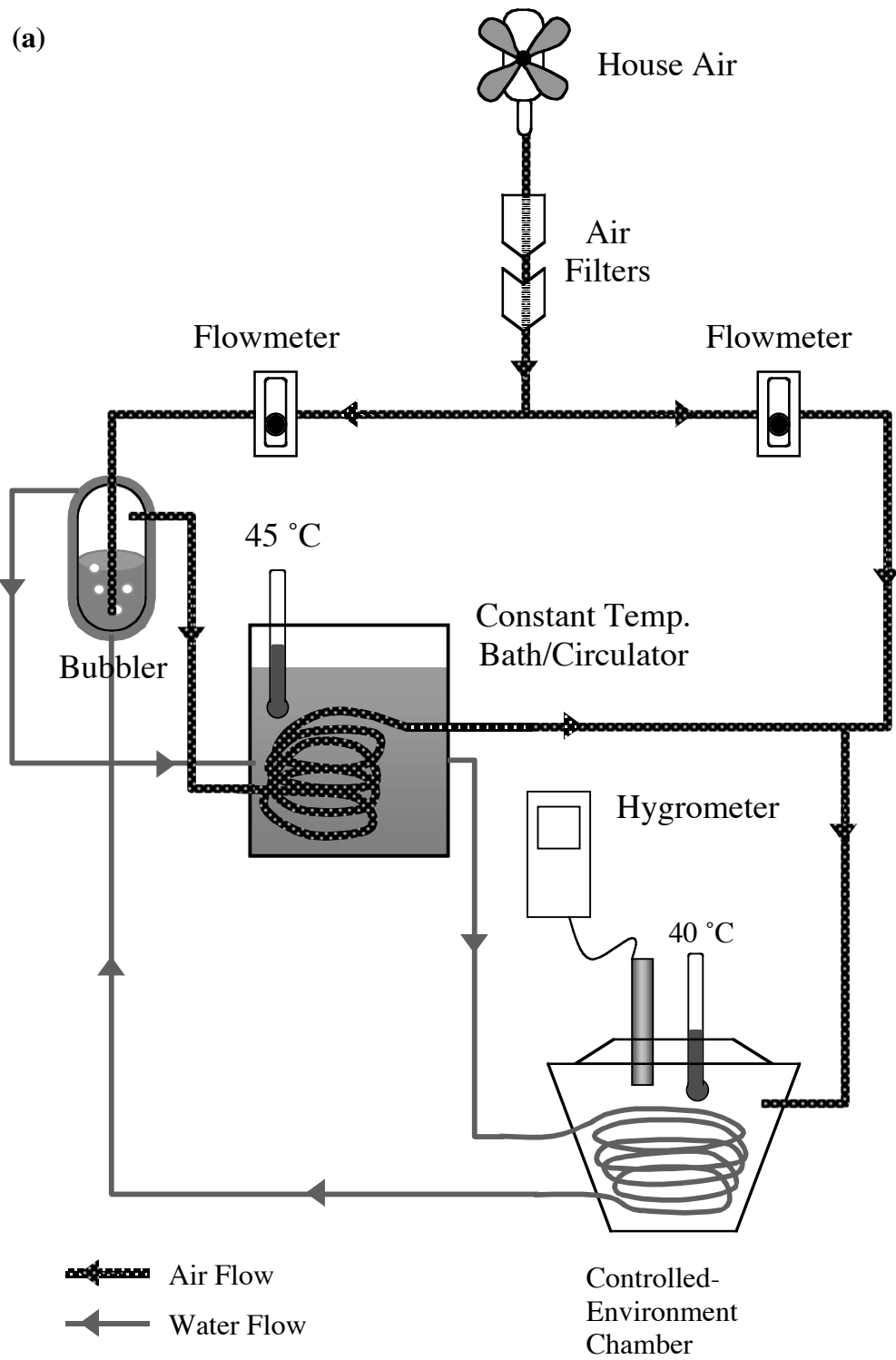
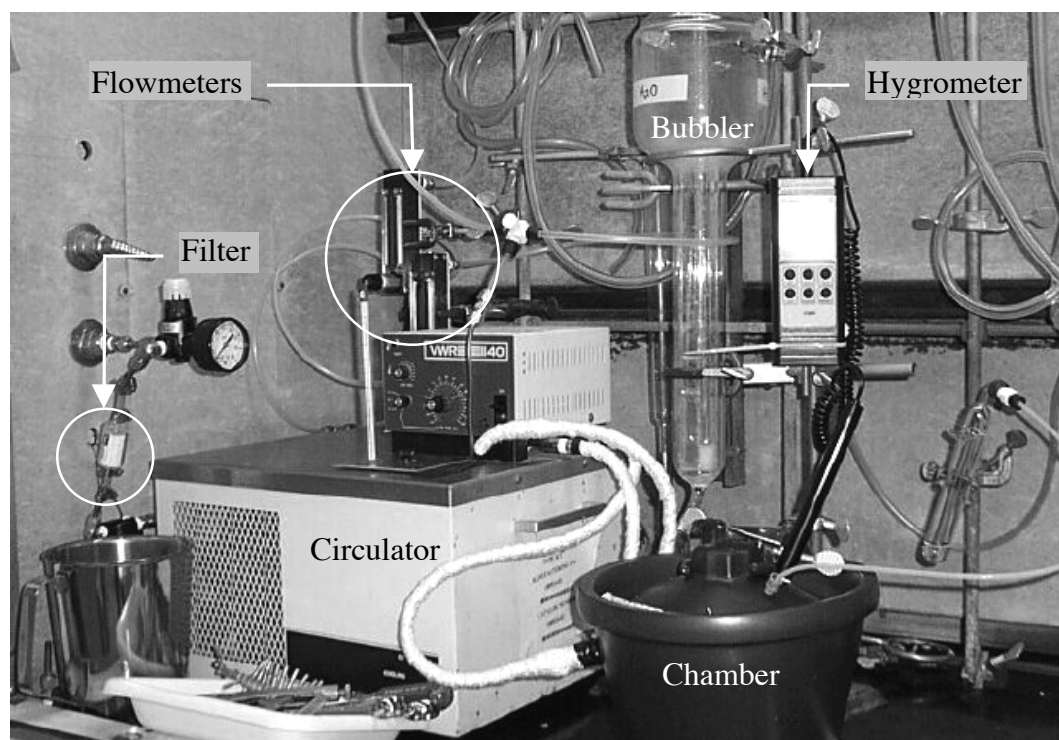


Figure 4.4

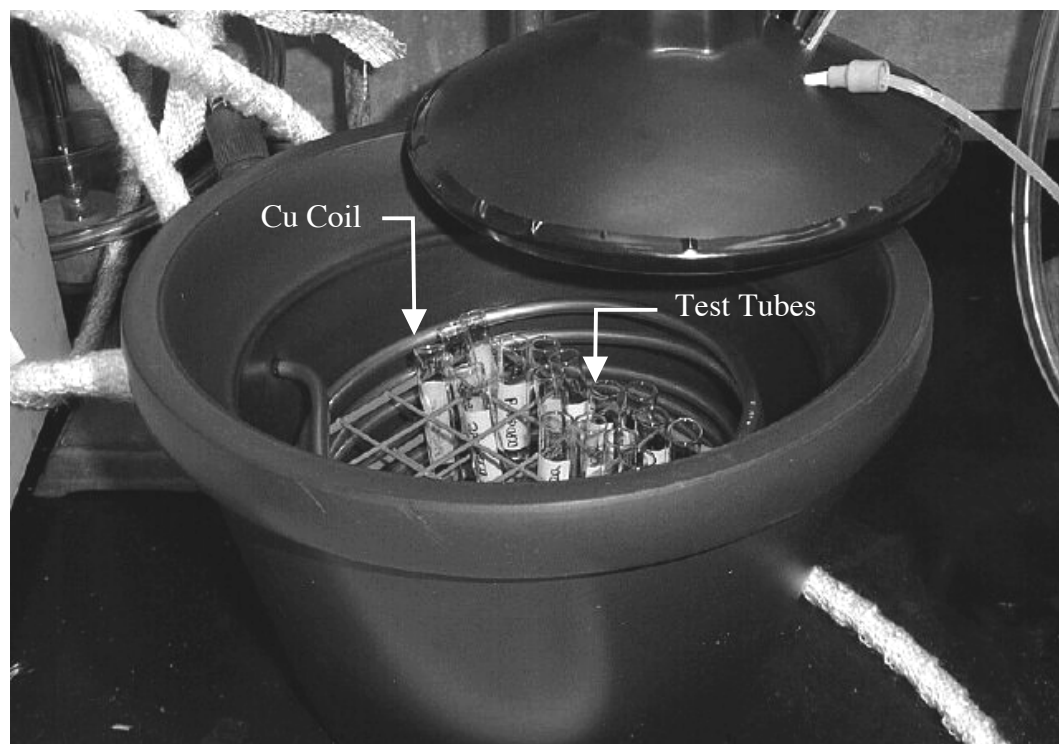
(a) A schematic of the controlled-environment chamber for sample storage under an elevated temperature and relative humidity condition. Filtered house air is split into two paths; one path is designed to saturate the air with water vapor at 45 °C, and the other path delivers original dry filtered house air. With the aid of flowmeters, two paths were then combined to create an environment with an air temperature of 40 °C and 80–90% relative humidity. (b) A photograph of the controlled-environment setup. (c) A detailed photograph showing the interior of the chamber. The 45 °C water was circulated through the Cu tubing to provide heating inside the chamber. The test tubes were used to hold the samples being stored.



(b)



(c)



3. Results

3.1. Surface Modifications

Four monomers were used for the modification of Si(111) surfaces using ring-opening metathesis polymerization (ROMP) method. The x-ray photoelectron spectroscopy (XPS) results suggest that both norbornene and dicyclopentadiene (DCPD) were successfully polymerized on the Si surfaces, but surface-initiated ROMP did not produce detectable polymer overlayers with either cyclooctadiene (COD) or cyclooctatetraene (COT) monomer.

The surface modification process was monitored and verified using XPS. Figure 4.5 displays the XP spectra obtained at each step of the surface modification process. A successful etching procedure produces an H-terminated Si surface with a clean spectrum showing large Si 2p and Si 2s peaks at 99 eV and 149 eV binding energies. The smaller peaks present at successive intervals of 17.5 eV binding energy higher than the main Si 2p and 2s peaks were plasmon loss peaks, and were characteristic of Si surfaces.^{49,50} Small signals due to adventitious carbon and oxygen were often observed at 284.6 eV (C 1s) and 532 eV (O 1s). The presence of adventitious carbonaceous material on the silicon surface was a result of wet chemical etching and subsequent brief handling of samples in air.^{51,52} The lack of signal in the 101 to 104 eV region of the Si 2p high-resolution XP spectra collected with each survey scans suggested that the oxygen signal observed in survey spectra was not due to silicon oxide.

Figure 4.5b shows the representative spectrum of a chlorinated Si surface. Addition peaks were observed at 270 eV and 200 eV binding energies, which correspond to Cl 2s and Cl 2p peaks.⁴³ Attachment of the terminal olefin was confirmed by the disappearance of the Cl peaks and the concomitant increase in magnitude of the C 1s

peak in the XP survey spectrum (Figure 4.5c). However, a direct evidence of the attachment of Ru catalyst could not be confirmed using XPS data (Figure 4.5d). The subsequent growth of polymer film and a set of control experiments offered indirect but convincing confirmations of the catalyst addition reaction.

3.1.1. Polynorbornene-Terminated Si

For most polynorbornene films, growth of polymer was evidenced by the disappearance of the Si signals and the formation of an overlayer that only displayed C peaks in the XP survey scan (Figure 4.5e). When a low concentration (<0.09 M) norbornene solution was used for polymerization, the observed survey spectrum displayed an increase in magnitude of the C 1s peak while the magnitude of the Si peaks were decreased but still visible. The surfaces of polynorbornene-terminated Si made with higher concentration (2.44 M) norbornene solutions appeared colorful and the films were thick enough to be visible by the naked eyes. Both C3 olefin- and C5 olefin-polynorbornene-terminated Si surfaces were successfully made.

3.1.2. PolyDCPD-Terminated Si

The ROMP of DCPD was monitored using XPS in the same fashion as described. Figure 4.6 displays the XPS survey spectra of polyDCPD-terminated Si surfaces made from four different DCPD concentrations (0.27 M, 0.45 M, 0.98 M, and 2.5 M in dichloromethane). The ROMP of DCPD did not produce polymer films of the same thickness as seen with norbornene. Although the ring-strains of norbornenes and DCPDs are very similar, the larger size of a DCPD monomer unit could hinder monomer diffusion to the surface-bound Ru initiator and thus limit the film thickness. However, the film thickness could still be controlled by the monomer concentrations as evidenced by XPS analysis. When polymerized DCPD is subject to heat (~40–50 °C) the remaining cyclic olefins are expected to undergo ring-opening polymerization and cross-link with

neighboring olefins. Although the cross-linking property of polyDCPD on surfaces was not investigated in this work, considering that the surface-bound polyDCPD chains are immobilized, the extent of cross-linkage could be somewhat limited.

3.1.3. ROMP of COD and COT

Attempts to produce polyCOD- and polyCOT (polyacetylene)-terminated surfaces were unsuccessful. The XP spectra showed no polymer formation on the Si surfaces following either immersion of **1**-modified Si into COD or immersion of **2**-modified Si into COT. Since COT is less strained than norbornene and COD, a more powerful Ru catalyst **2** was used in place of **1** to initiate the ROMP reaction. The XP survey spectrum shows no significant increase in the magnitude of C 1s peak. To be certain that the catalyst **2** would initiate ROMP on a surface in a similar fashion as the catalyst **1**, it was used to polymerize norbornene (2.44 M in 1,2-dichloroethane). The resulting XP spectrum revealed a large C 1s peak and no detectable Si peaks, and a colorful film was seen on the surface as observed when norbornene was polymerized using catalyst **1**. Thus, surface bound **2** was successful at polymerize norbornene.

3.1.4. Control Experiments

Additional experiments were performed to establish that (i) the polymerization of norbornene was directly initiated by **1**, and (ii) the resulting polymer film was attached covalently to the Si surface. When an olefin-terminated Si substrate was exposed to a solution of norbornene, no polymer was observed by XPS (Figure 4.7a). In addition, when an H-terminated Si surface was exposed to a solution of norbornene, no polymer formed and the XPS signals showed only Si and a very small amount of adventitious C and O (Figure 4.7b). Exposure of an H-terminated Si surface to a solution of **1** followed by exposure to a solution of norbornene produced a polymer that did not persist on the Si surface after washing with dichloromethane (Figure 4.7c). These wet chemical

experiments imply that the technique described in this chapter did in fact produce covalently attached polymeric films on the Si surface, and the polymerization could not occur without the Ru initiators.

Figure 4.5

XP survey spectra of (a) H-terminated Si, (b) Cl-terminated Si, (c) allyl-terminated Si, (d) allyl-terminated Si after immersing in a solution of **1** for 3 hours, and (e) covalently attached polynorbornene on Si. Spectra in (a)–(d) were normalized relative to the intensity of the Si 2p peak. Typical Si 2p:C 1s:O 1s peak ratios were (a) 1:(0.35 ± 0.06):(0.36 ± 0.09), (b) 1:(0.54 ± 0.03):(0.39 ± 0.04) (average of 2 spectra), (c) 1:(0.82 ± 0.22):(0.68 ± 0.22), and (d) 1:(2.04 ± 0.26):(0.46 ± 0.12) (average of 2 spectra).

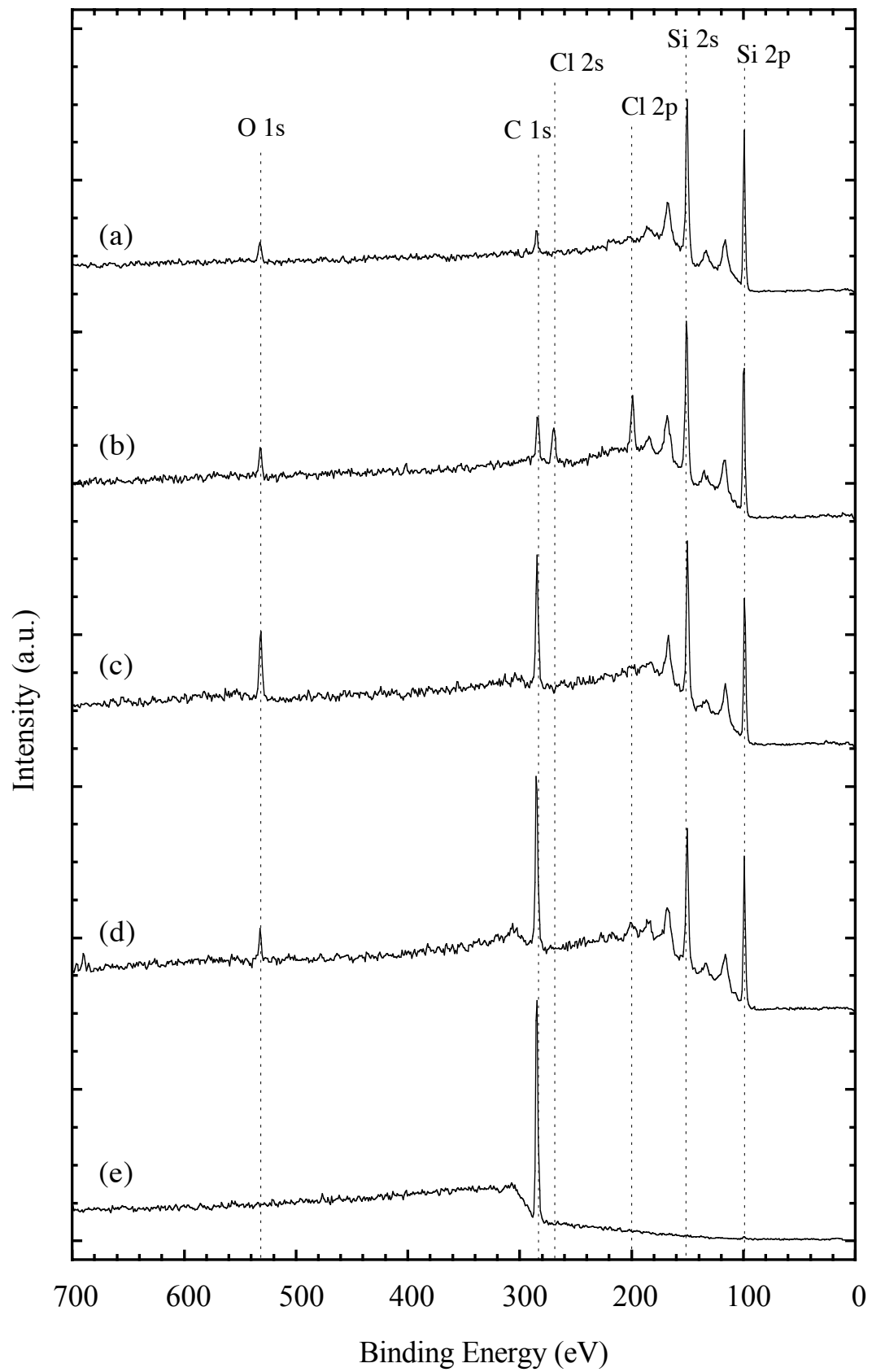


Figure 4.6

XP survey spectra of polyDCPD-terminated Si made from solutions of (a) 0.27 M, (b) 0.45 M, (c) 0.98 M, and (d) 2.5 M DCPD in dichloromethane. All spectra were normalized relative to the intensity of the Si 2p peak.

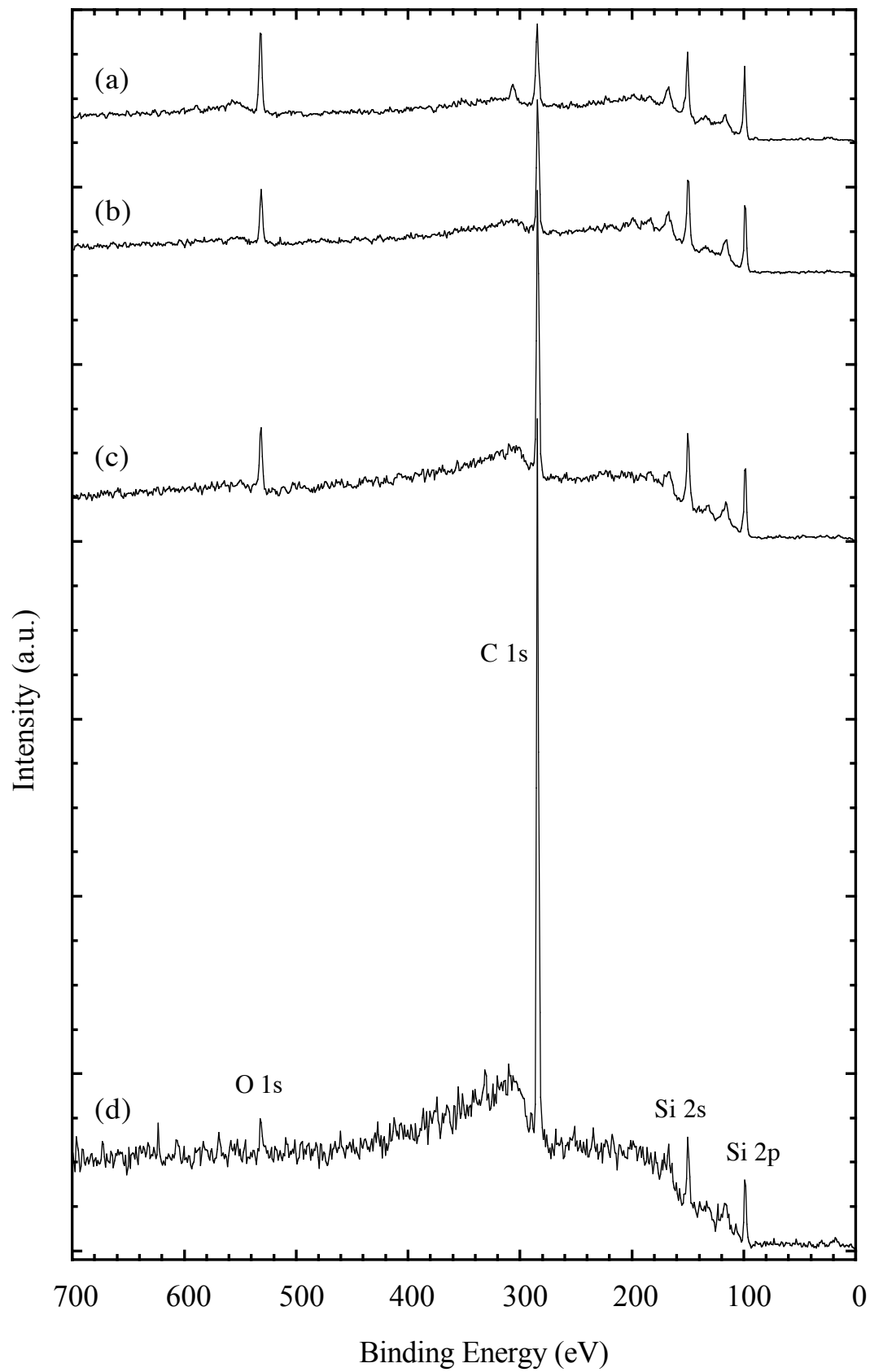
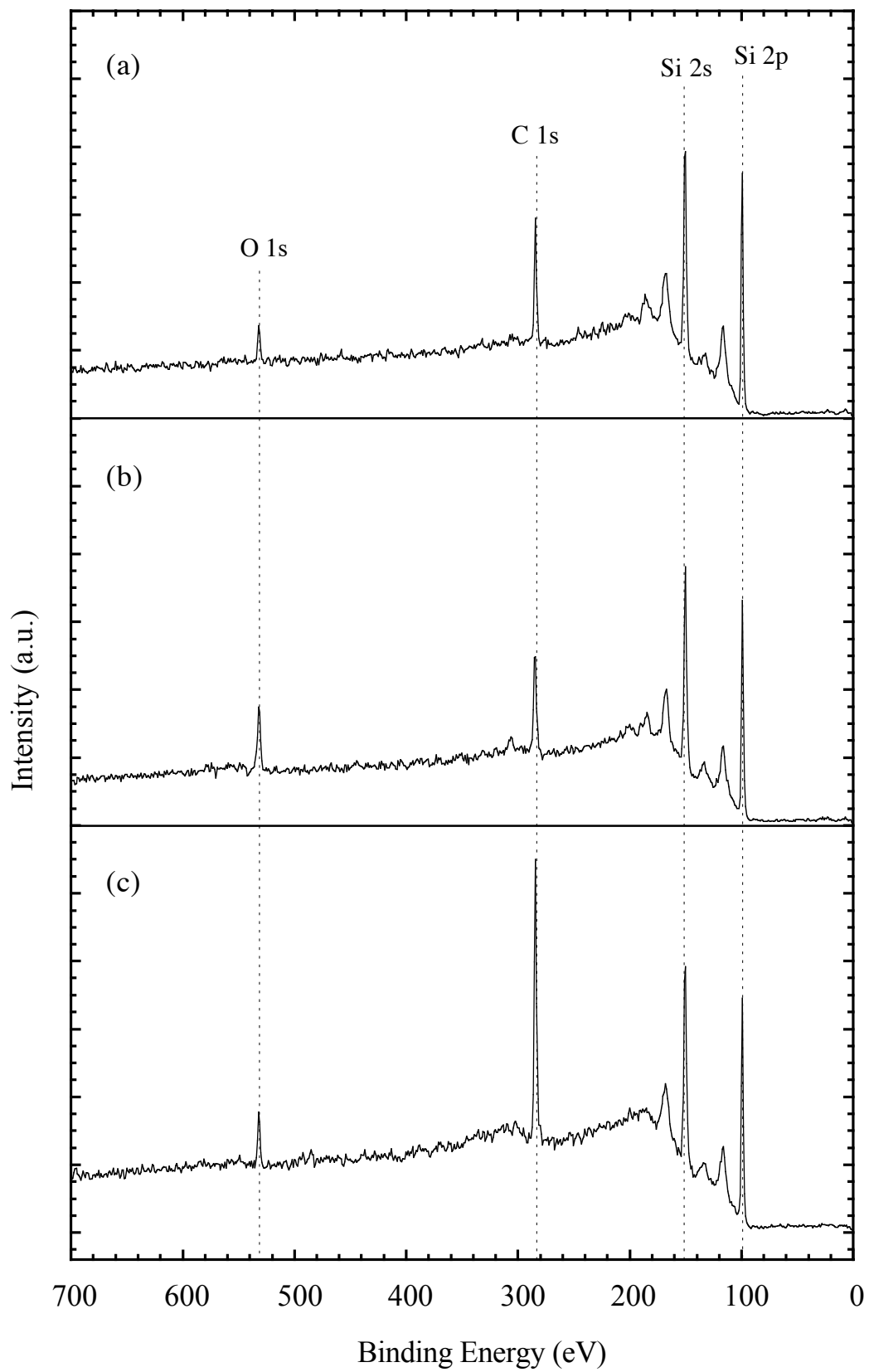


Figure 4.7

XP survey spectra of (a) C₄ olefin-terminated Si following immersion in norbornene (2.44 M in 1,2-dichloroethane) for 30 min, (b) H-terminated Si following immersion in the same norbornene solution for 30 min, and (c) H-terminated Si after being immersed in a solution of **1** and then norbornene. All surfaces were rinsed with anhydrous dichloromethane after each immersion. All spectra were normalized relative to the intensity of the Si 2p peak. Compare to the spectrum of a polynorbornene-terminated Si (Figure 4.5e), spectra (a)–(c) indicated no significant polymer growth after these surface treatments.



3.2. Surface Characterizations

3.2.1. Polymer Thickness Measurements

Because ROMP initiated by **1** is a controlled polymerization process,^{53,54} different film thicknesses could be obtained by varying the concentration of monomer solutions. Table 4.2 summarizes the thicknesses of several polynorbornene films produced at a fixed reaction time (30 min) in response to variation in the concentration of monomer in the solution. The standard deviation in the ellipsometrically derived thickness measured at several different spots for each sample was usually less than $\pm 10\%$ of the mean thickness value, indicating that the polymer film covered the entire Si substrate. Figure 4.8a displays a partial surface profile of a polynorbornene-terminated Si made from a 2.44 M norbornene solution. This profile includes a feature representing the area of a spatula scrape as shown in the SEM image of the same sample (see Figure 4.8b). The upward spikes at the edges of the feature are most likely the result of polymer being pushed and piled up to the sides when the spatula was used to scraped off small amount of polymer on the surface. The center parts of these features are very flat and smooth, which is a good indication of that being the flat surface of a Si substrate. The measured profilometric thicknesses of both 0.15 M and 0.45 M polynorbornene films were consistent with the ellipsometric data (Table 4.2). The polymer films formed using a 2.44 M solution were too thick for ellipsometric measurements, therefore only the profilometric result is reported.

3.2.2. Scanning Electron Microscopy

Figure 4.9 shows two top-view images of polynorbornene-terminated Si samples ([norbornene] = 0.15 M and 2.44 M) at 500 \times magnification. A thinner polynorbornene overlayer appears to be smoother compared to a thicker overlayer at the same

magnification. This observation is consistent with the polymer thickness measurements displaying larger standard deviation values when thicker polymer films were grown. Figure 4.10 displays a SEM image of the cross section of a sample (obtained after immersion of a **1**-treated, allyl-terminated Si sample into a 2.44 M solution of norbornene in 1,2-dichloroethane for 30 min) at 1500 \times magnification. A film thickness of $5.3 \pm 0.2 \mu\text{m}$ over a distance of $75 \mu\text{m}$ was measured from this micrograph. The SEM images also indicate that the Si substrates were indeed covered entirely by polynorbornene. The estimated thickness of the polymer film from SEM images of two samples at 1500 \times magnification is $5.6 \pm 0.06 \mu\text{m}$, which agrees with the thickness of $5.39 \pm 0.14 \mu\text{m}$ measured using profilometry.

Table 4.2

Dependence of the polymer overlayer thickness on the concentration of norbornene in the solution.

[Norbornene] (M)	Thickness ^a (Å)	Number of Samples	Number of Spots Per Sample
0.01	9 ± 2	4	6
0.05	83 ± 65	2	7
0.09	119 ± 16	4	6
0.15	297 ± 40	2	7
0.18	374 ± 130	6	5
0.27	1130 ± 38	5	6
0.45	2230 ± 410	2	7
2.44	53920 ± 1420 ^b	1	2

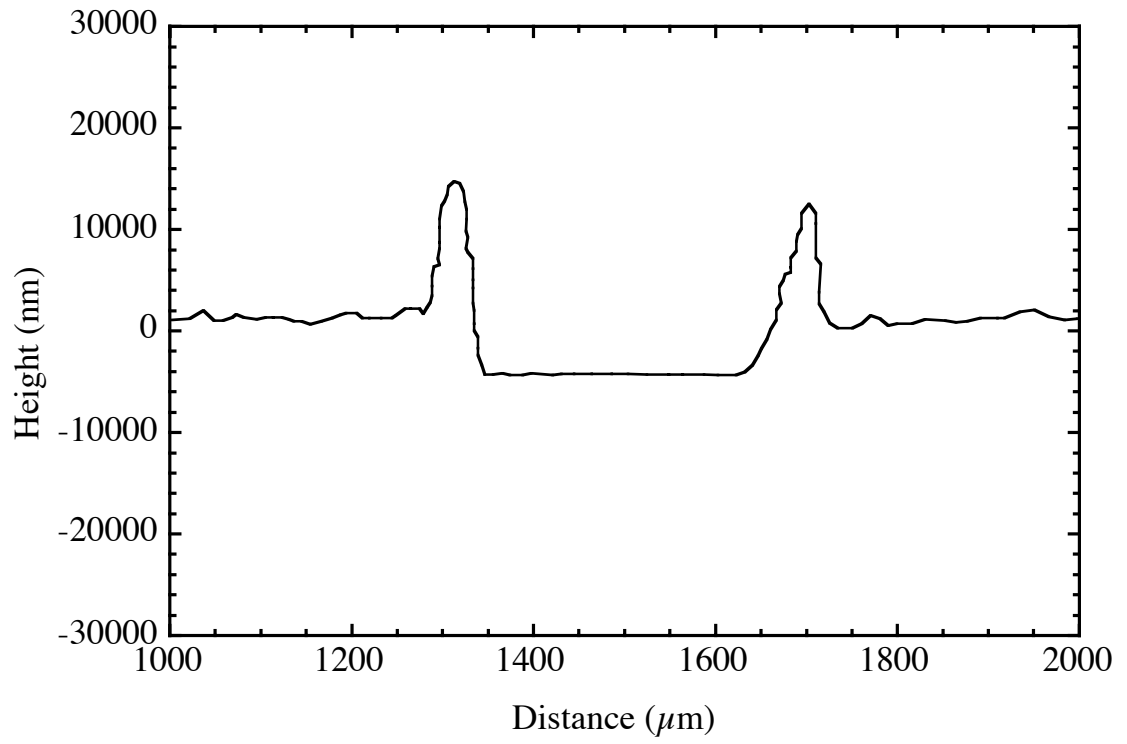
^a Each thickness value is an average of measurements on the corresponding number of samples, with the reported number of spots measured on each sample. The standard deviation between measurements at different locations of one sample was usually less than ±10% of the mean film thickness value of that sample; therefore the quoted standard deviation in this table only reflects the differences in polymer overlayer thickness between different samples or different experimental trials.

^b The thickness data of this sample was acquired using profilometry.

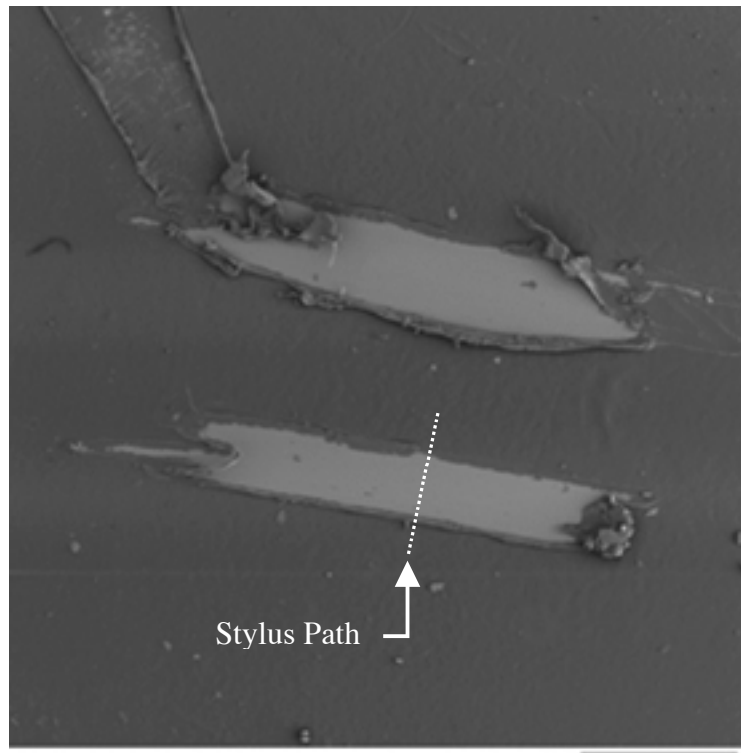
Figure 4.8

(a) A partial surface profile of a polynorbornene-terminated Si surface obtained through profilometry. The polymer overlayer was grown using 2.44 M norbornene solution. By scraping a thin strip of polymer off the substrate and running the stylus of a profilometer across the scratch, the height of examined surface was plotted and the thickness of the overlayer could be determined from the height difference between the bottom of the feature and the surrounding polymer layer. The surface feature plotted corresponds to one of the spatula scraps shown in (b), which is a SEM image of the same surface at 30× magnification. The spatula scratches revealed the bare surface of the Si substrate.

(a)



(b)

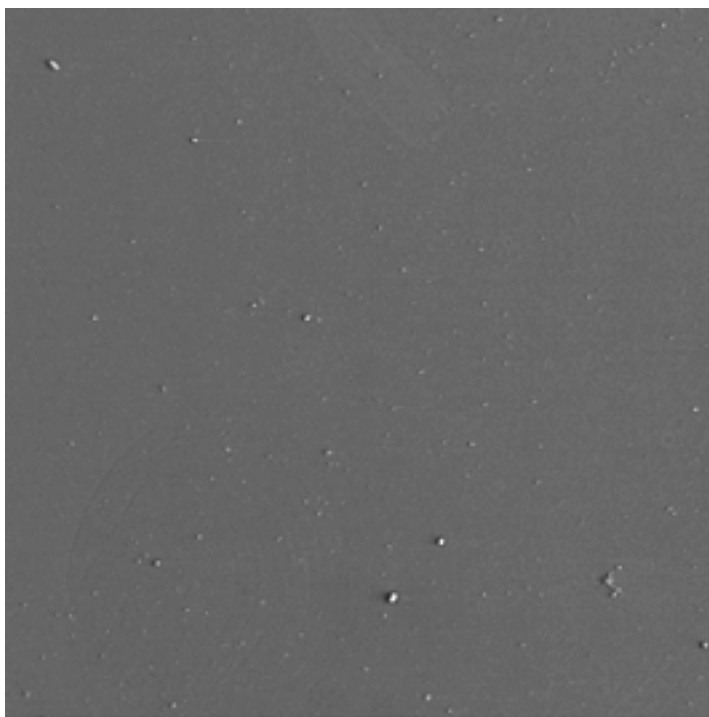


800 μm 30X

Figure 4.9

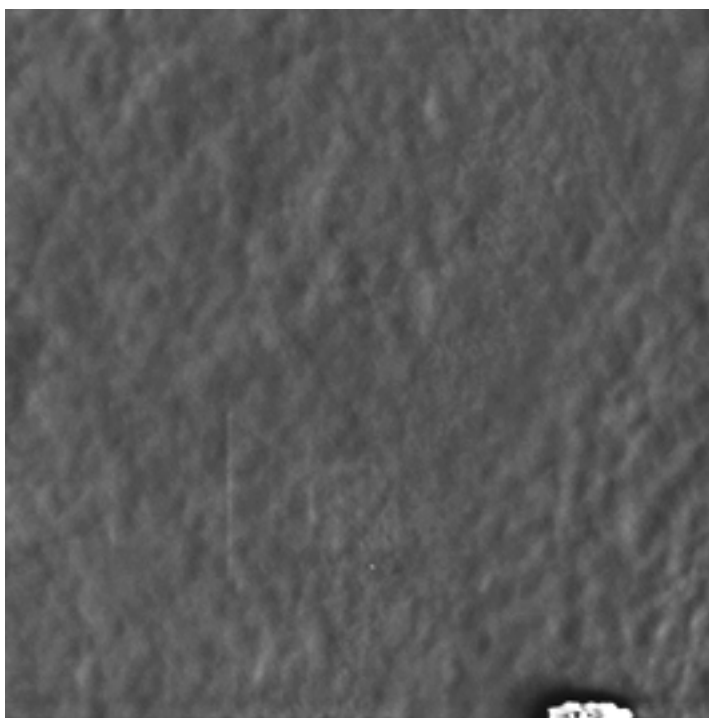
SEM top-view images of two polynorbornene-terminated Si surfaces made from (a) 0.15 M and (b) 2.44 M norbornene/1,2-dichloroethane solutions. The overlayer thicknesses of two samples were $271 \pm 20 \text{ \AA}$ and $53920 \pm 1420 \text{ \AA}$, respectively. The samples with thicker polymer overlayers were found to have larger standard deviations in their thickness measurements, which can be explained by the SEM image showing a rougher surface for a thicker overlayer under the same magnification.

(a)



50 μm 500×

(b)



50 μm 500×

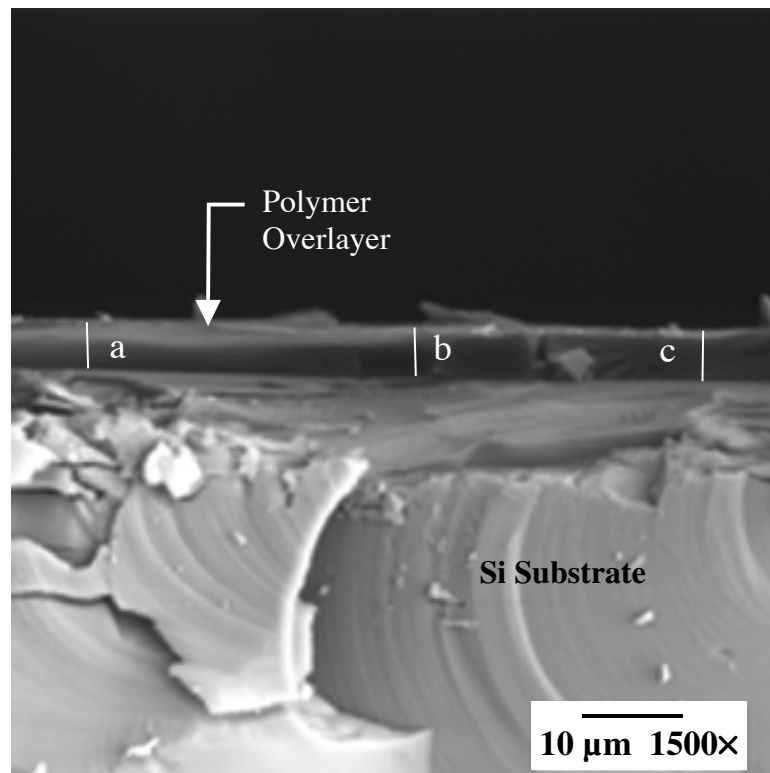


Figure 4.10

A cross-sectional SEM image of a polynorbornene-covered Si surface at 1500 \times magnification. The polymer film covered the entire Si substrate, and the estimated film thicknesses at points a, b, and c from the SEM image are 5.0, 5.5, and 5.4 μm , respectively. These values are in good agreement with the mean polymer thickness of $5.39 \pm 0.14 \mu\text{m}$ that was determined for the same sample using profilometry.

3.3. Photoconductivity Decay Measurements

Time-resolved photoconductivity decay curves of various surfaces are included in the following sections. Each shown curve is the average of 128 decays, and is fit by a single exponential to extract the time constant for carrier recombination. The observed lifetime τ can be related to the bulk lifetime τ_b and the surface recombination velocity S through this equation.⁵⁵⁻⁵⁷

$$\frac{1}{\tau} = \frac{1}{\tau_b} + \frac{2S}{d} \quad (4.1)$$

where d is the sample thickness. The S reported in this chapter were calculated assuming that the experimentally observed lifetime is dominated by surface recombination with no contribution from charge-carrier recombination in the bulk ($\tau_b = \infty$); therefore, it is important to note that the reported S values represent the upper limit to the true S values.

3.3.1. C3 Olefin-Terminated and C3 Olefin-Polymer-Terminated Si Surfaces

Figure 4.11 displays the transient photoconductivity decay behaviors of C3 olefin-terminated, C3 olefin-polybornene-terminated, and C3 olefin-polyDCPD-terminated Si surfaces in an $N_2(g)$ ambient. The initial photoconductivity decays of C3-olefin-modified Si surfaces were relatively slow, with a mean charge-carrier lifetime of $250 \pm 60 \mu s$. When a C3 olefin-terminated surface was further modified with either polybornene or polyDCPD, the mean charge-carrier lifetime decreased to $230 \pm 90 \mu s$ and $170 \pm 10 \mu s$, respectively. The initial S values of these three surfaces were calculated using Equation 4.1. Assuming an infinite bulk lifetime and $d = 294 \mu m$, the upper bound S values were determined to be $59 \pm 10 \text{ cm s}^{-1}$, $64 \pm 20 \text{ cm s}^{-1}$, and $88 \pm 3 \text{ cm s}^{-1}$, respectively.

Figure 4.12 shows the time-dependent mean carrier lifetimes of all three surfaces in air (21 °C and 7% R.H.). The Si surfaces modified with C3 olefin were not able to preserve the initial surface quality and the lifetime value dropped very quickly following the air exposure. Furthermore, the polymer overlayers were found to be ineffective in protecting the Si surfaces after the C3 olefin layers had failed, and the mean lifetimes of both polynorbornene- and polyDCPD-modified surfaces also decreased, though not as quickly as the C3 olefin-terminated Si. Within 5 hours after the C3 olefin-terminated samples were exposed to the air, the mean lifetime had already exhibited a fivefold decrease to $<50 \mu\text{s}$. Within 30 hours of the air exposure, the mean carrier lifetimes of polymer-terminated surfaces had also dropped to about $50 \mu\text{s}$. After being exposed to the air for 120 hours, C3 olefin- and C3 olefin-polyDCPD-terminated surfaces were found to have S values of $1600 \pm 500 \text{ cm s}^{-1}$ and $610 \pm 40 \text{ cm s}^{-1}$. The degradation of the lifetime for a C3 olefin-terminated surface was very similar to that of an unmodified Si-H surface in air. Although the polymer overlayers added some protection to the C3 olefin-modified surfaces, a more effective olefin linker could improve the charge-carrier lifetime at the modified Si/air interface.

The mean carrier lifetimes of three different C3 olefin-polynorbornene overlayer thicknesses were also investigated to determine the optimal polymer thickness that worked the best to preserve the modified surfaces after exposure to the air. Although the thicker polymer layer was expected to be a better barrier against oxidation of the Si surface which leads to an increased surface defects, no such trend was observed when the time-dependent S of samples made using 0.09 M, 0.18 M, and 0.27 M norbornene solutions were plotted. For following experiments, polynorbornene overlayers made from a 0.27 M solution were used unless otherwise stated.

3.3.2. Effects of Olefin Linker Chain Length

Several terminal olefin linkers were investigated for the purpose of finding the one that is capable of generating well-preserved surfaces for further modification steps. Figure 4.13 displays the time dependence of the mean carrier lifetimes of Si surfaces modified with mixed methyl/allyl (50%:50%, C1/C3 olefin), C3 olefin, C5 olefin, and C6 olefin linkers. With a suspicion that C3 olefin did not provide enough surface coverage to prevent the oxidation of Si substrate, an olefin layer of better surface coverage was desired for improving the charge-carrier lifetime of modified Si. Since methyl groups are small enough to bind to neighboring Si atoms on the surface,⁵⁸ and may be able to fill in the pinholes created by C3 olefin modification, methyl Grignard was mixed in with allyl Grignard to generate mixed C1/C3 olefin-terminated surfaces. However, this mixed linker was not able to preserve the carrier lifetime, and the S value of this surface following 90 hour of air exposure was almost as high as that of an unmodified Si-H and a C3 olefin-terminated surfaces in air, though the rate of the lifetime degradation was slower for this type of surfaces.

Longer terminal olefin linkers are more flexible and the tilted chains might be able to cover the surface better. When C6 olefin-terminated Si was found to have a stable carrier lifetime after 120 hours of air exposure, C5 olefin-terminated surfaces were also tested. Interestingly, the C5 olefin termination not only had a stable lifetime, but it also exhibited a longer carrier lifetime. The C5 olefin was therefore used as a linker for all further surface modifications.

3.3.3. C5 Olefin-Terminated and C5 Olefin-Polymer-Terminated Si Surfaces

Figure 4.14 displays the transient photoconductivity decay behaviors of C5 olefin-terminated, C5 olefin-polybornene-terminated, and C5 olefin-polyDCPD-terminated Si surfaces in an $N_2(g)$ ambient. The initial photoconductivity decays of C5-

olefin- modified Si surfaces yielded a mean charge-carrier lifetime of $360 \pm 10 \mu\text{s}$. Further modification with either polynorbornene or polyDCPD produced surfaces with mean carrier lifetimes of $200 \pm 30 \mu\text{s}$ and $190 \pm 110 \mu\text{s}$, which are comparable with the C5 olefin-polymer modified surfaces. The initial S values of these three surfaces were calculated using Equation 4.1. Assuming an infinite bulk lifetime and $d = 294 \mu\text{m}$, the upper bound S values were determined to be $41 \pm 1 \text{ cm s}^{-1}$, $75 \pm 10 \text{ cm s}^{-1}$, and $76 \pm 50 \text{ cm s}^{-1}$, respectively.

Figure 4.15 plots the time dependence of the carrier lifetime of each surface in air under different temperature/humidity conditions. Although the carrier lifetime of C5 olefin-terminated Si was very high initially, it was decreasing very slowly over the course of 700 hours, and the lifetime drop was slightly more pronounced for samples stored under the $40 \text{ }^\circ\text{C}/80\text{--}90\%$ R.H. condition (Figure 4.15a). On the other hand, the carrier lifetimes of both C5 olefin-polynorbornene- and C5 olefin-polyDCPD- terminated surfaces were not affected by the storage condition, and the surfaces recombination velocities remained low after almost one month of air exposure.

Figure 4.16 shows the time-dependent mean carrier lifetimes of all three surfaces in air ($21 \text{ }^\circ\text{C}$ and 7% R.H.); after prolong exposure of these surfaces in air, all still exhibited low surface recombination velocities. Following 650 hours of air exposure, the S values were found to be $49 \pm 7 \text{ cm s}^{-1}$, $61 \pm 10 \text{ cm s}^{-1}$, and $66 \pm 10 \text{ cm s}^{-1}$ for C5 olefin-terminated, C5 olefin-polynorbornene-terminated, and C5 olefin-polyDCPD-terminated Si surfaces, respectively. The capability for C5 olefin-polymer-terminated surfaces to reserve the initial low surface-defect-density of the modified Si surfaces in $\text{N}_2(\text{g})$ was confirmed.

Figure 4.17 displays the time-dependent mean carrier lifetimes of all three surfaces in air under an elevated temperature and humidity environment ($40 \text{ }^\circ\text{C}$ and $80\text{--}90\%$ R.H.). Again, after prolonged exposure of these surfaces in air, all still exhibited low surface recombination velocities. Following 600 hours of air exposure, the S values

were found to be $70 \pm 30 \text{ cm s}^{-1}$, $51 \pm 8 \text{ cm s}^{-1}$, and $59 \pm 10 \text{ cm s}^{-1}$ for C5 olefin-terminated, C5 olefin-polynorbornene-terminated, and C5 olefin-polyDCPD-terminated Si surfaces, respectively. Although the mean carrier lifetime of the C5 olefin surfaces has decreased slightly after 600 hours of air exposure, it was still comparable with the lifetimes of both polymer-terminated Si. The time-dependent carrier lifetime and surface recombination velocity data are summarized in Table 4.3.

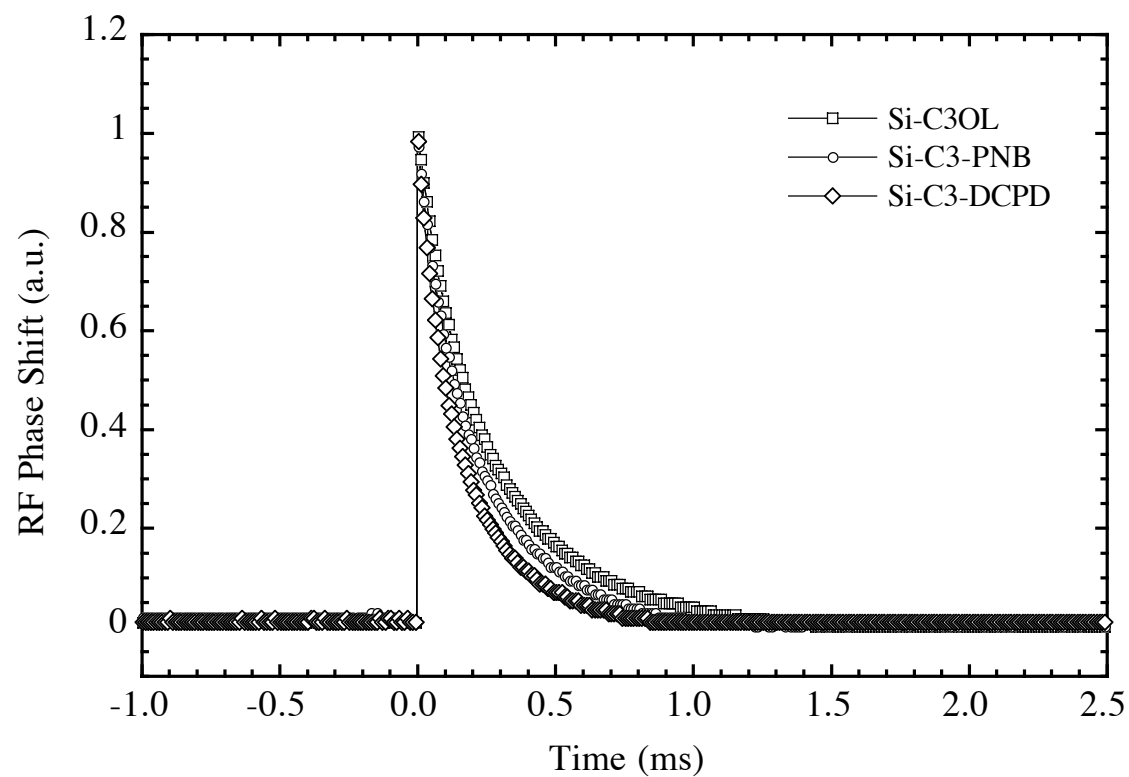


Figure 4.11

Time-resolved photoconductivity decay curves of C3 olefin-terminated (squares), C3 olefin-polynorbornene-terminated (circles), and C3 olefin-polyDCPD-terminated (diamonds) Si surfaces in an $N_2(g)$ ambient. The decays were obtained under high-level injection conditions. Single exponential fits to these decay curves (not shown) yielded a time constant of $280 \mu s$, $220 \mu s$, and $168 \mu s$, respectively.

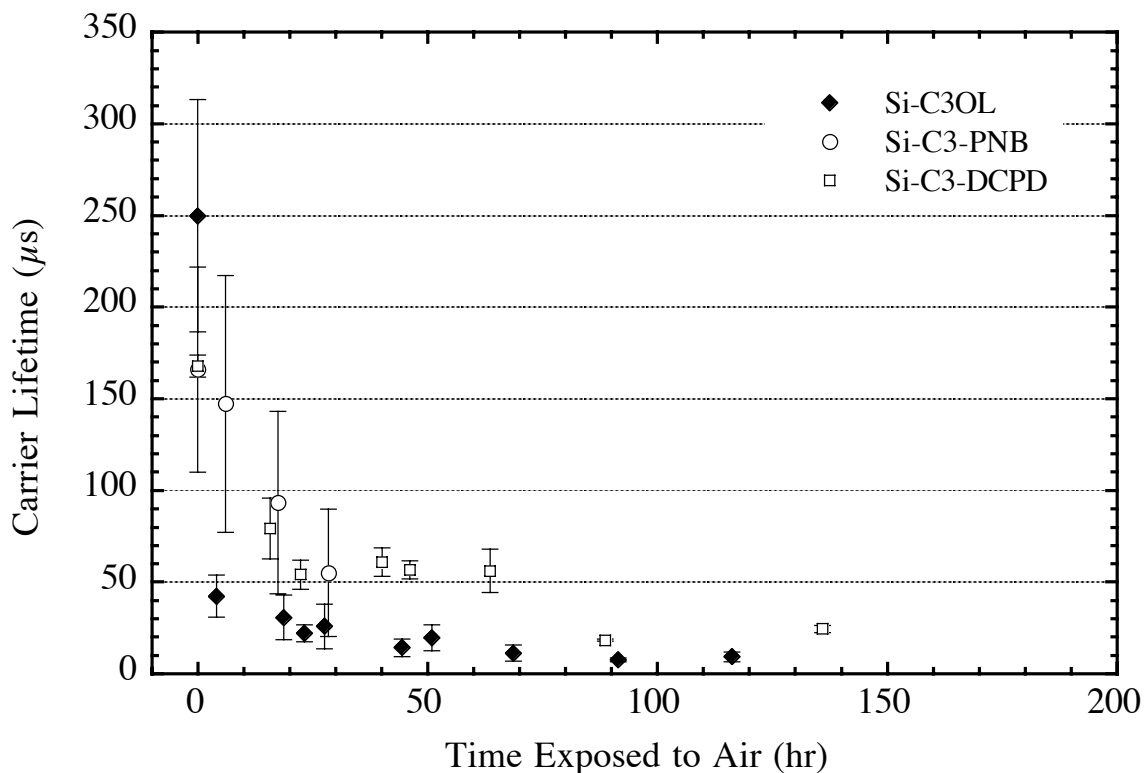


Figure 4.12

Time dependence of the mean carrier lifetimes for C3 olefin-terminated (filled diamonds), C3 olefin-polynorbornene-terminated (open circles), and C3 olefin-polyDCPD-terminated (open squares) Si in air. The samples were stored in a dark controlled environmental chamber with an air temperature of 21 °C and a relative humidity of 7% in between measurements. All data were acquired under high-level injection conditions. The error bars represent the standard deviations for measurements obtained from at least three samples.

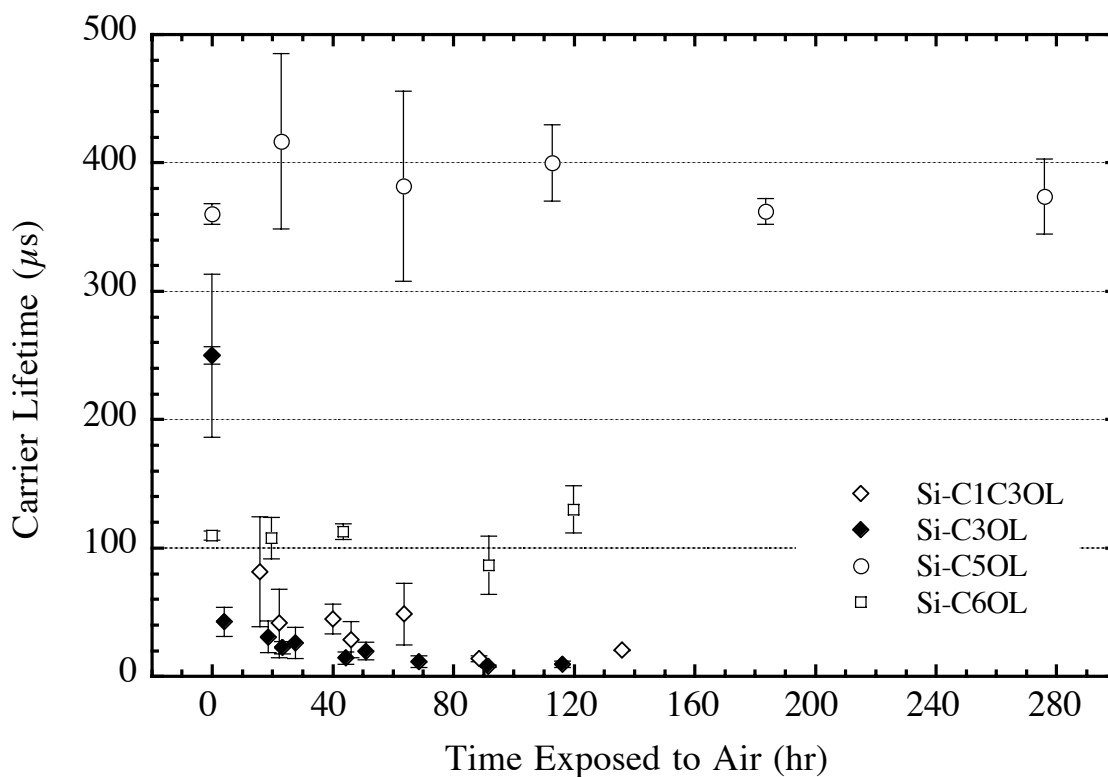


Figure 4.13

Time dependence of the mean carrier lifetimes for mixed methyl/C3 olefin-terminated (open diamonds), C3 olefin-terminated (filled diamonds), C5 olefin-terminated (open circles), and C6 olefin-terminated (open squares) Si surfaces in air. The samples were stored in a dark controlled environmental chamber with an air temperature of 21 °C and a relative humidity of 7% in between measurements. All data were acquired under high-level injection conditions. The error bars represent the standard deviations for measurements obtained from at least two samples.

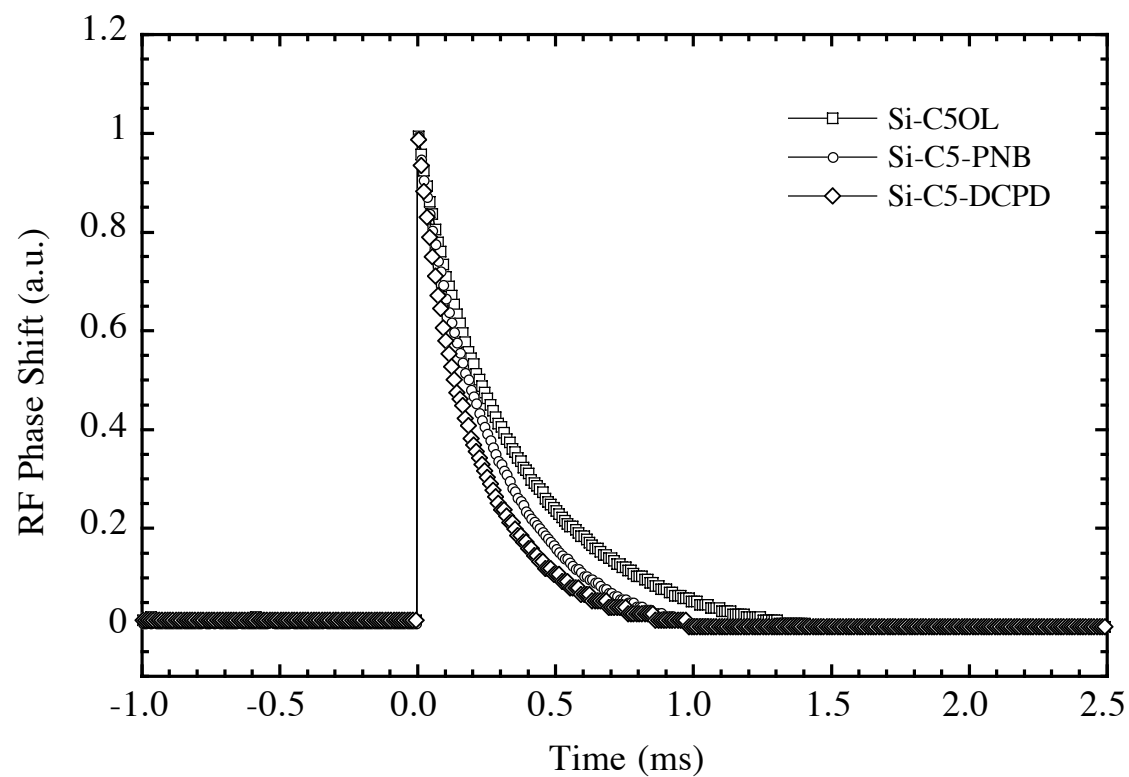


Figure 4.14

Time-resolved photoconductivity decay curves of C5 olefin-terminated (squares), C5 olefin-polynorbornene-terminated (circles), and C5 olefin-polyDCPD-terminated (diamonds) Si surfaces in an $N_2(g)$ ambient. The decays were obtained under high-level injection conditions. Single exponential fits to these decay curves (not shown) yielded a time constant of $366 \mu s$, $273 \mu s$, and $219 \mu s$, respectively.

Figure 4.15

Time dependence of the mean carrier lifetimes for (a) C5 olefin-terminated, (b) C5 olefin-polynorbornene-terminated, and (c) C5 olefin-polyDCPD-terminated Si surfaces exposed to elevated temperature/humidity (open circles) and low temperature/humidity (filled circles) conditions. The samples exposed to the elevated temperature/humidity condition were stored in a dark controlled environmental chamber with an air temperature of 40 °C and a relative humidity of 80–90% in between measurements. The samples exposed to the low temperature/humidity condition were stored in a dark controlled environmental chamber with an air temperature of 21 °C and a relative humidity of 7% in between measurements. All data were acquired under high-level injection conditions. The error bars represent the standard deviations for measurements obtained from at least two samples.

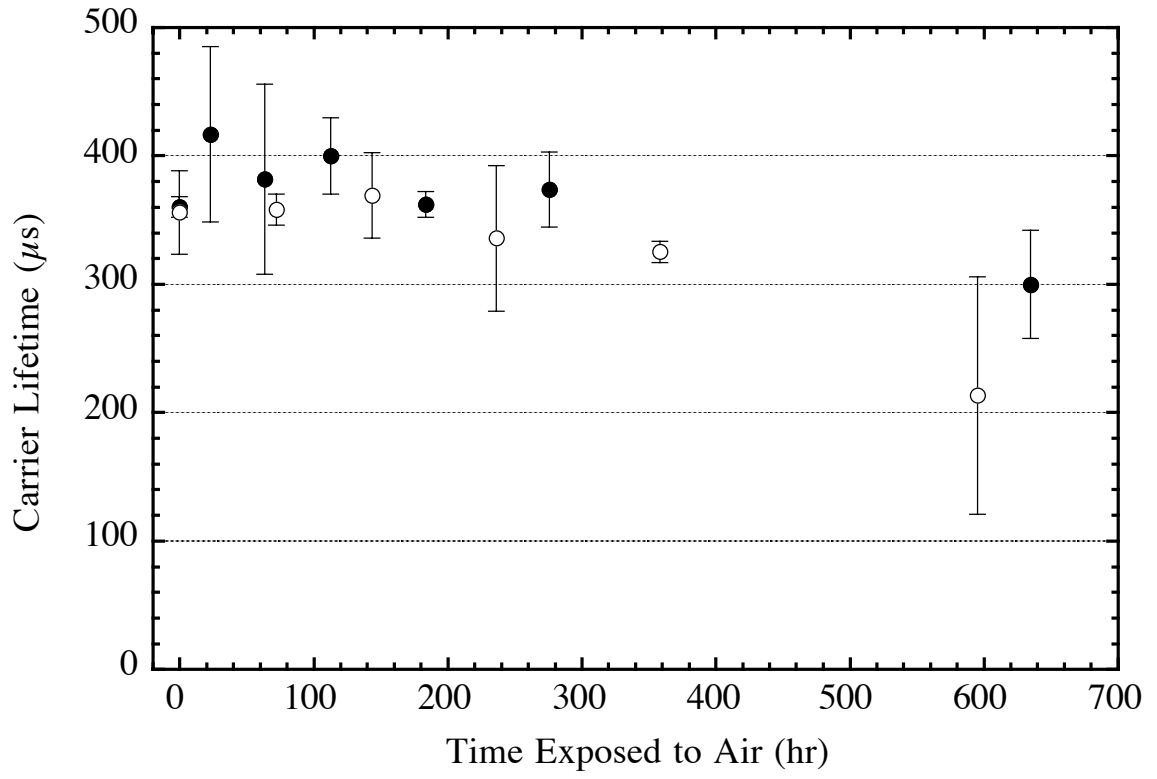
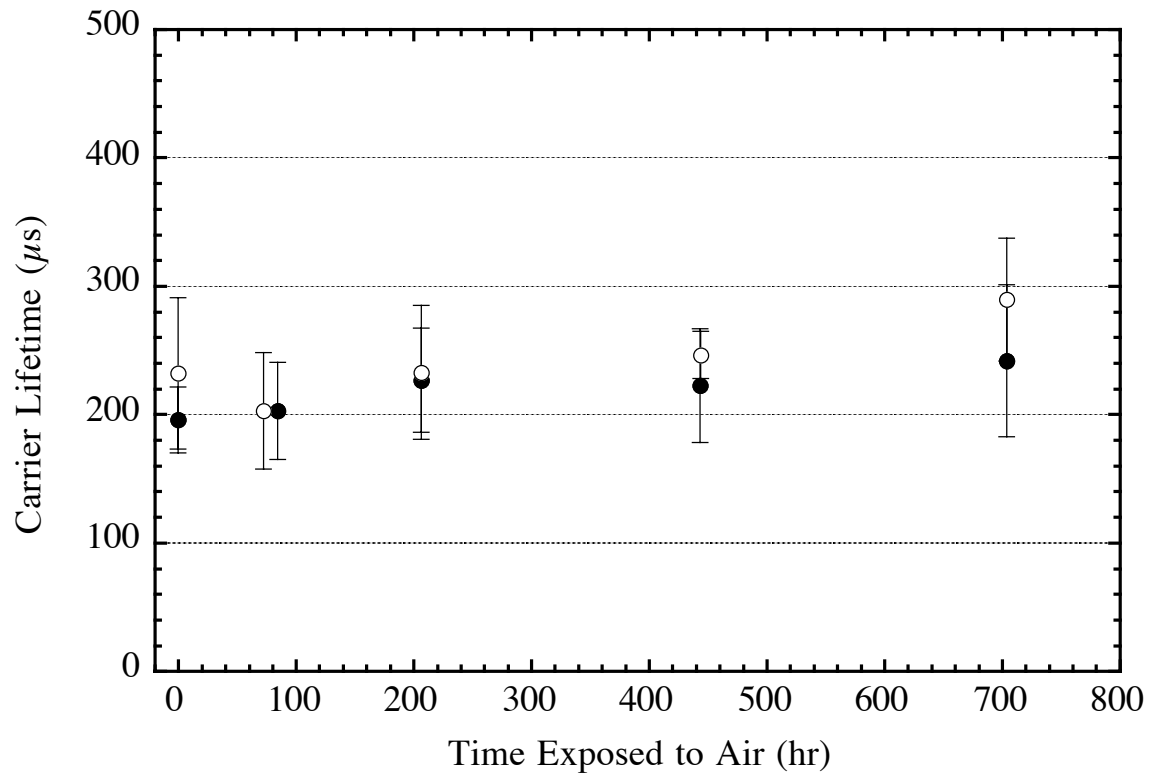
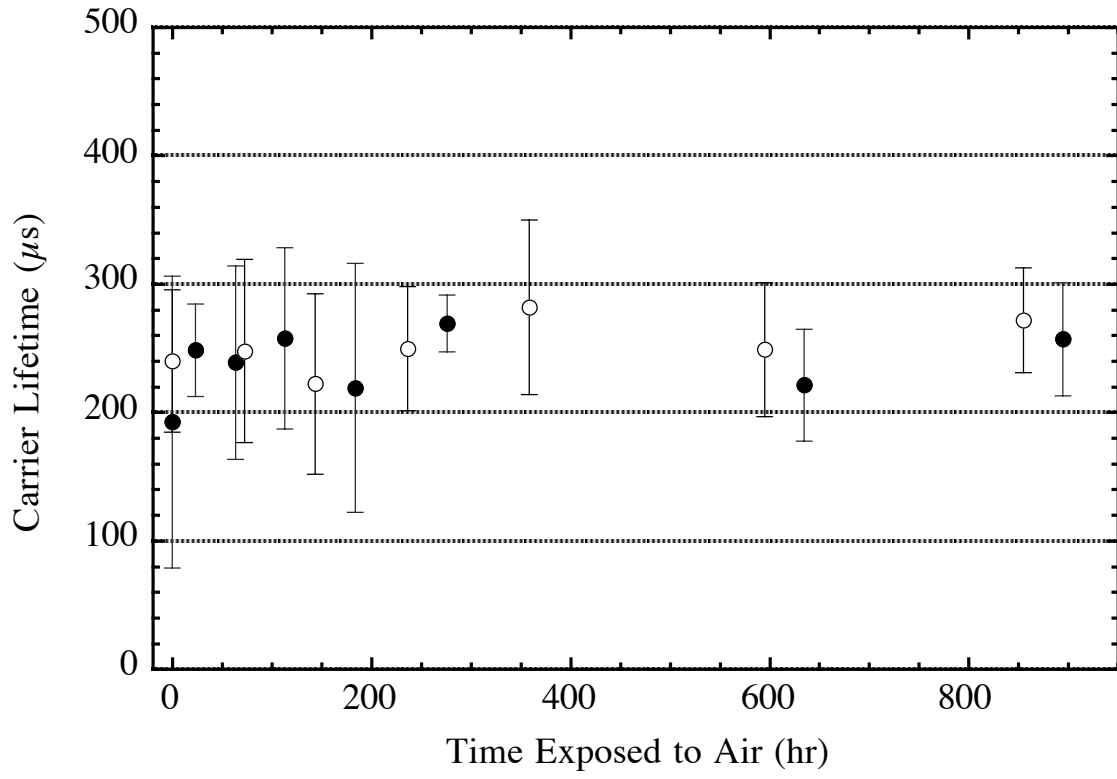


Figure 4.15a

**Figure 4.15b**

**Figure 4.15c**

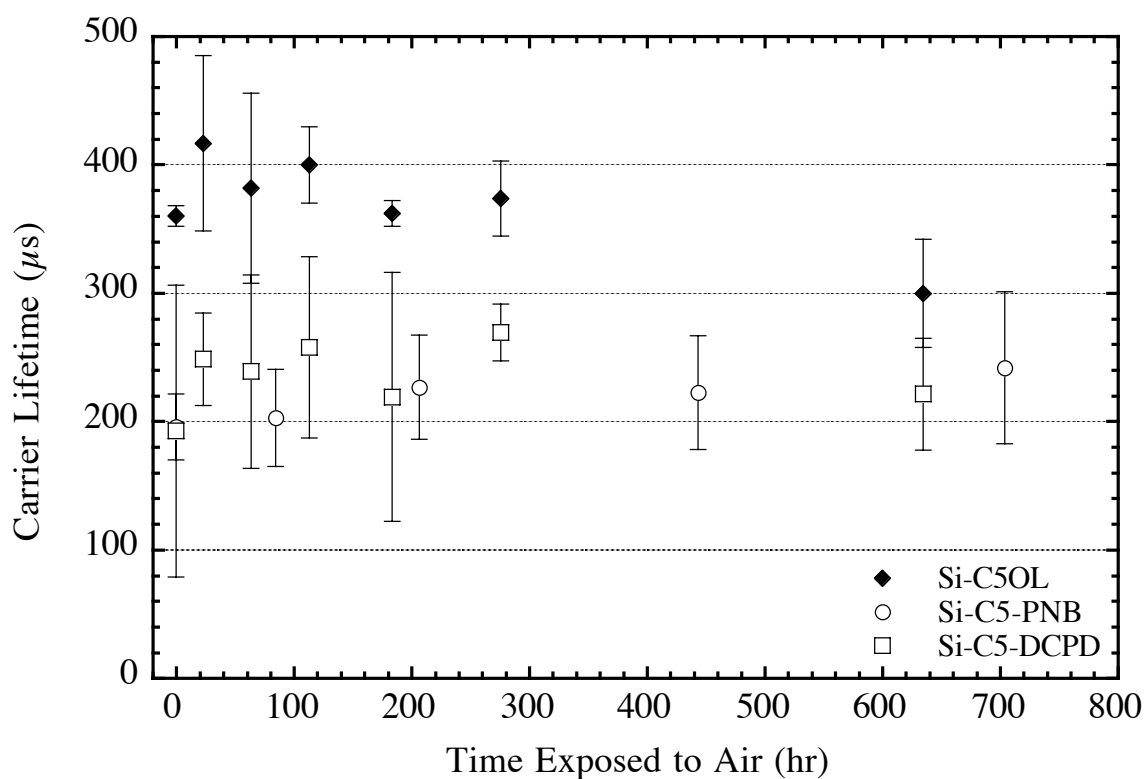


Figure 4.16

Time dependence of the mean carrier lifetimes for C5 olefin-terminated (filled diamonds), C5 olefin-polynorbornene-terminated (open circles), and C5 olefin-polyDCPD-terminated (open squares) Si surfaces exposed to a low temperature/humidity condition. The samples were stored in a dark controlled environmental chamber with an air temperature of 21 °C and a relative humidity of 7% in between measurements. All data were acquired under high-level injection conditions. The error bars represent the standard deviations for measurements obtained from at least two samples.

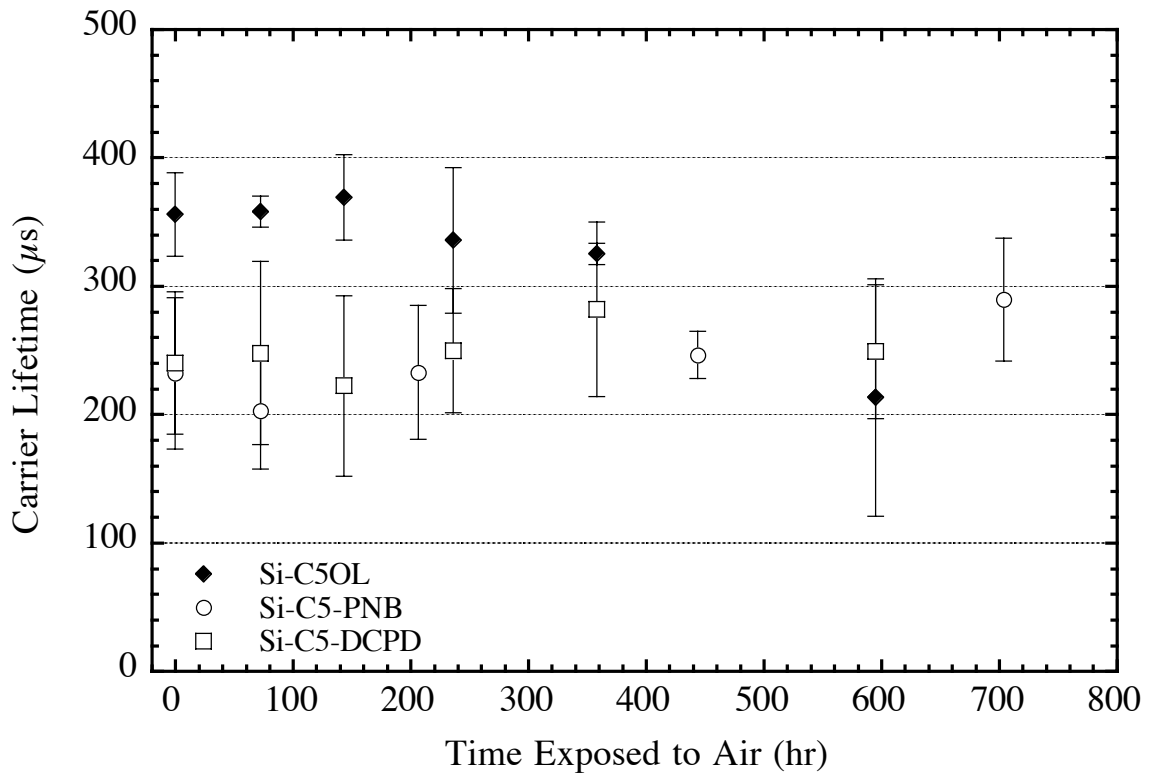


Figure 4.17

Time dependence of the mean carrier lifetimes for C5 olefin-terminated (filled diamonds), C5 olefin-polynorbornene-terminated (open circles), and C5 olefin-polyDCPD-terminated (open squares) Si surfaces exposed to an elevated temperature/humidity condition. The samples were stored in a dark controlled environmental chamber with an air temperature of 40 °C and a relative humidity of 80–90% in between measurements. All data were acquired under high-level injection conditions. The error bars represent the standard deviations for measurements obtained from at least two samples.

Table 4.3

Time-dependent measured carrier recombination lifetimes and surface recombination velocities for various modified Si surfaces. Values of S were calculated assuming an infinite bulk lifetime.

Overlayer	τ (μs)	S (cm s^{-1})	τ (μs)	S (cm s^{-1})	τ (μs)	S (cm s^{-1})
21 °C/7% R.H.	In N₂(g)		After ~30 hr in Air		After ~120 hr in Air	
C3 olefin	250 ± 60	59 ± 10	26 ± 10	570 ± 270	9 ± 3	1600 ± 500
C3 olefin-polynorbornene	230 ± 90	64 ± 20	55 ± 30	270 ± 170	-- ^a	-- ^a
C3 olefin-polyDCPD	170 ± 10	88 ± 3	57 ± 5	260 ± 20	24 ± 2	610 ± 40
21 °C/7% R.H.	In N₂(g)		After ~150 hr in Air		After ~600 hr in Air	
C5 olefin	360 ± 10	41 ± 1	360 ± 10	41 ± 1	300 ± 40	49 ± 7
C5 olefin-polynorbornene	200 ± 30	75 ± 10	230 ± 40	65 ± 10	240 ± 60	61 ± 10
C5 olefin-polyDCPD	190 ± 110	76 ± 50	220 ± 100	67 ± 30	220 ± 40	66 ± 10
40 °C/80–90% R.H.	In N₂(g)		After ~150 hr in Air		After ~600 hr in Air	
C5 olefin	360 ± 30	41 ± 4	370 ± 30	40 ± 4	210 ± 90	70 ± 30
C5 olefin-polynorbornene	230 ± 60	63 ± 20	230 ± 50	63 ± 10	290 ± 50	51 ± 8
C5 olefin-polyDCPD	240 ± 60	61 ± 10	220 ± 70	66 ± 20	250 ± 50	59 ± 10

^a Charge-carrier lifetimes were not measured.

3.4. Time-Dependent XPS Studies: Oxidation of Modified Si surfaces in Air

While C5 olefin- and C5 olefin-polymer-terminated surfaces exhibited stable carrier lifetimes when exposed to air under both low temperature/humidity and elevated temperature/humidity conditions, the effectiveness of the overlayers in preventing the oxidation of Si substrates was investigated by monitoring the change in the Si 2p region of XP high-resolution spectra. The thickness of the SiO₂ layer was calculated from the relative areas of the bulk Si 2p and oxidized Si 2p peaks in the high-resolution XP spectrum. A simple substrate–overlayer model was adapted for this calculation.^{59,60}

$$d = \lambda_{\text{ov}} \sin \theta \left\{ \ln \left[1 + \left(\frac{I_{\text{Si}}^0}{I_{\text{ov}}^0} \right) \left(\frac{I_{\text{ov}}}{I_{\text{Si}}} \right) \right] \right\} \quad (4.2)$$

where d is the oxide overlayer thickness, λ_{ov} is the attenuation factor through the oxide overlayer, θ is the angle of the incident x-ray beam from the sample surface, $I_{\text{Si}}^0/I_{\text{ov}}^0$ is an instrumental normalization factor related to the ratio of the signals expected for pure Si vs pure SiO₂ and $I_{\text{ov}}/I_{\text{Si}}$ is the ratio of oxidized Si 2p to bulk Si 2p peak areas. Using 2.6 nm for the value of λ_{ov} ,⁶¹ 35° for θ , and 1.3 for $I_{\text{Si}}^0/I_{\text{ov}}^0$,⁶⁰ the thickness of the oxide layer was determined. The oxide coverage was then estimated using the SiO₂ monolayer thickness of 0.35 nm.⁶²

The time-dependent XP high-resolution spectra of C5 olefin- and C5 olefin-polyDCPD-terminated Si, oxidized under the two conditions described above, are displayed in Figure 4.18, Figure 4.19, Figure 4.20, and Figure 4.21. Oxidation of the Si substrates was observed for both types of surfaces. For C5 olefin modified surfaces, the amount of SiO₂ growth was determined to be 1.00 monolayer after 930 hours of oxidation in a 21 °C/7% R.H. condition and 0.21 monolayers in a 40 °C/80–90% R.H. condition for 860 hours. For C5 olefin-polyDCPD modified surfaces, the SiO₂ growth was 3.04

monolayers and 1.75 monolayers, respectively. In the case of oxidation under the 21 °C/7% R.H. condition, the amount of SiO₂ growth increased with the length of oxidation time. When samples were exposed to the elevated temperature/humidity condition, the oxide growth rate was faster but less overall oxide growth was observed for equivalent oxidation time lengths. For example, in an elevated temperature/humidity condition, the amount of oxide growth on a Si-C5 olefin-polyDCPD during the first 97 hours of oxidation was about the same as for the same type of surface to be oxidized in the low temperature/humidity condition for 384 hours. The oxide growth at an elevated temperature/humidity condition had also reached its maximum when the spectrum was collected after 97 hours of exposure time, while the oxide growth continued for samples stored under the low temperature/humidity condition. For comparison, the XP high-resolution spectra of the Si 2p region showing the time-dependent air oxidation of a hydrogen-terminated Si are displayed in Figure 4.22. The amount of oxide on the Si surface was determined to be 1.10 monolayers after 946 hours of air exposure at 21 °C/7% R.H. A summary of the oxide growth monitored by XPS is displayed in Table 4.4.

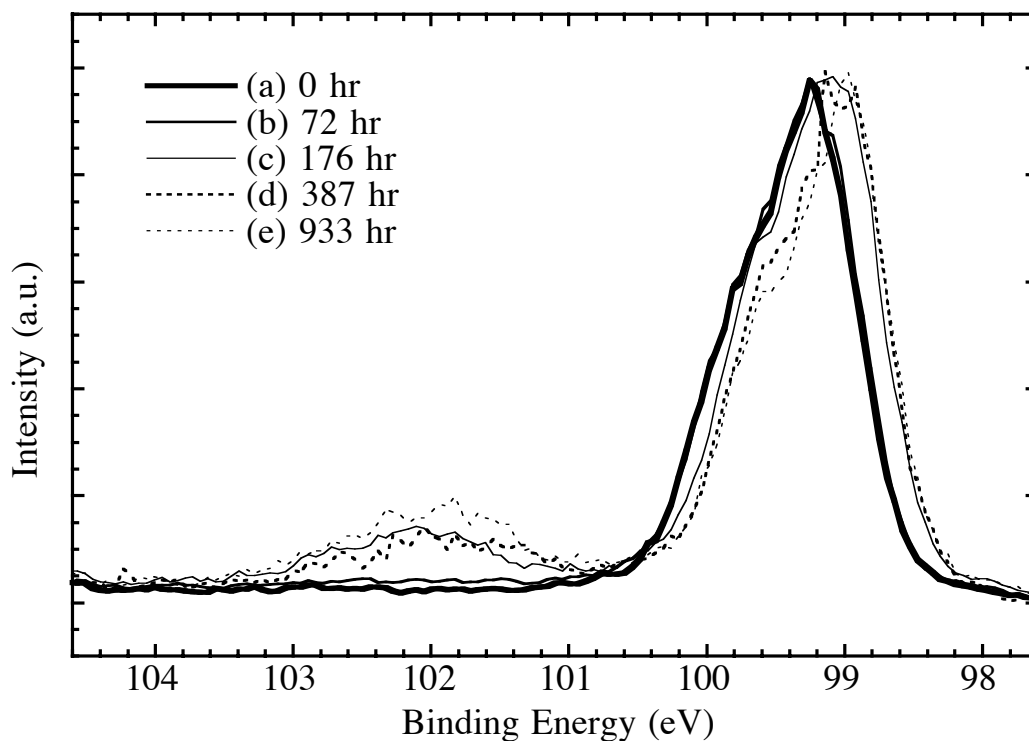


Figure 4.18

High-resolution XPS spectra of C5 olefin-terminated Si focusing on the Si 2p region collected (a) before exposing the surface to the air, (b) after 72 hours, (c) after 176 hours, (d) after 387 hours, and (e) after 933 hours of air exposure, under low temperature/humidity condition. The samples were stored in a dark controlled environmental chamber with an air temperature of 21 °C and a relative humidity of 7% in between measurements. These spectra were normalized relative to the intensity of bulk Si 2p peak (98.5–100.4 eV binding energies).

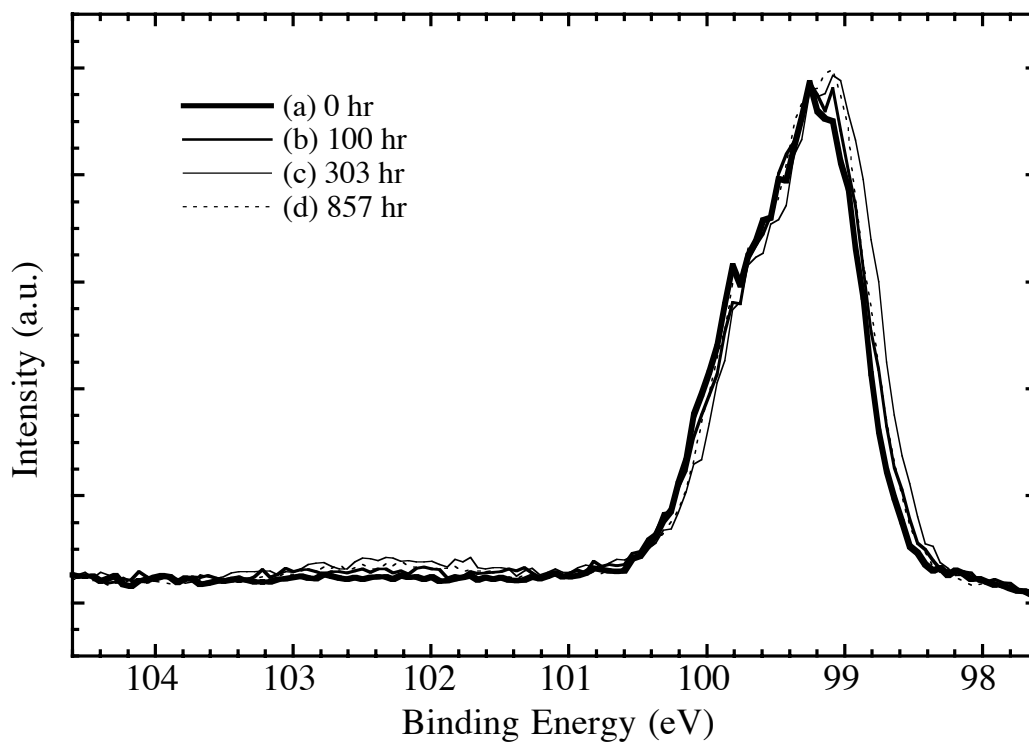


Figure 4.19

High-resolution XPS spectra of C5 olefin-terminated Si focusing on the Si 2p region collected (a) before exposing the surface to the air, (b) after 100 hours, (c) after 303 hours, and (d) after 857 hours of air exposure, under elevated temperature/humidity condition. The samples were stored in a dark controlled environmental chamber with an air temperature of 40 °C and a relative humidity of 80–90% in between measurements. These spectra were normalized relative to the intensity of bulk Si 2p peak (98.5–100.4 eV binding energies).

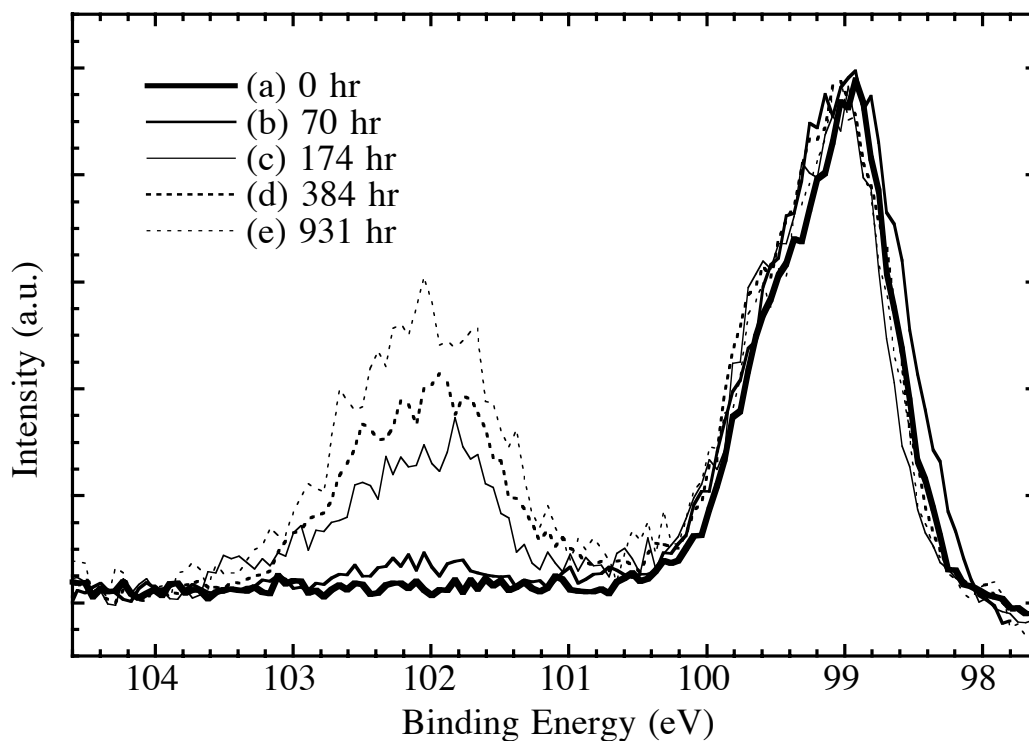


Figure 4.20

High-resolution XPS spectra of C5 olefin-polyDCPD-terminated Si focusing on the Si 2p region collected (a) before exposing the surface to the air, (b) after 70 hours, (c) after 174 hours, (d) after 384 hours, and (e) after 931 hours of air exposure, under low temperature/humidity condition. The samples were stored in a dark controlled environmental chamber with an air temperature of 21 °C and a relative humidity of 7% in between measurements. These spectra were normalized relative to the intensity of bulk Si 2p peak (98.5–100 eV binding energies).

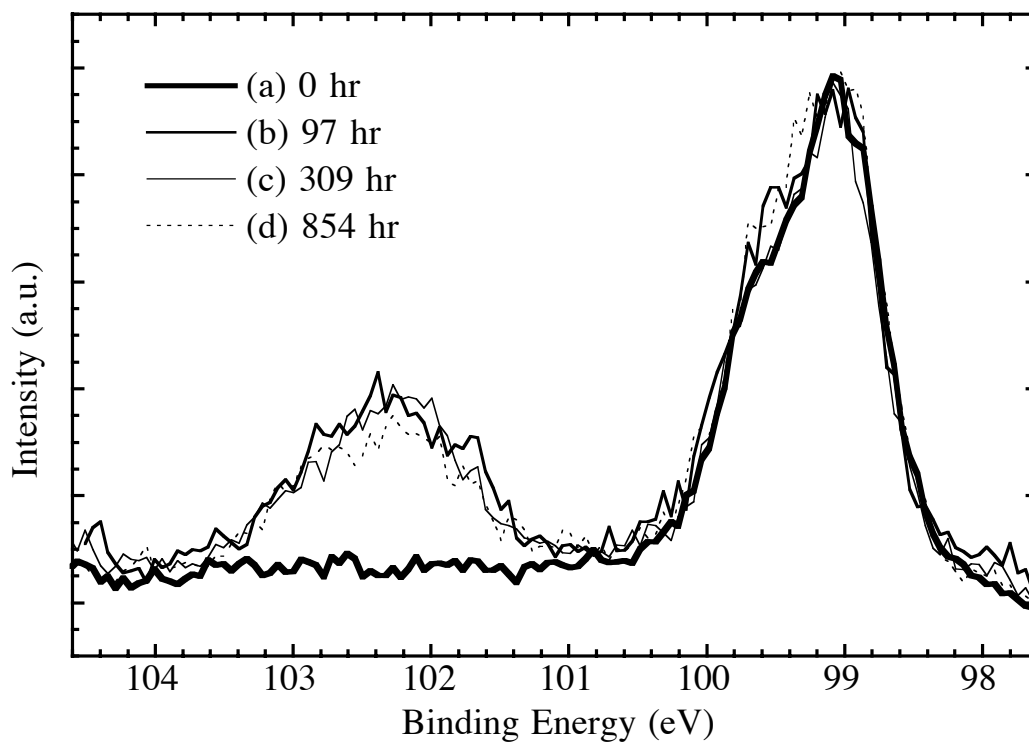


Figure 4.21

High-resolution XPS spectra of C5 olefin-polyDCPD-terminated Si focusing on the Si 2p region collected (a) before exposing the surface to the air, (b) after 97 hours, (c) after 309 hours, and (d) after 854 hours of air exposure, under elevated temperature/humidity condition. The samples were stored in a dark controlled environmental chamber with an air temperature of 40 °C and a relative humidity of 80–90% in between measurements. These spectra were normalized relative to the intensity of bulk Si 2p peak (98.5–100.4 eV binding energies).

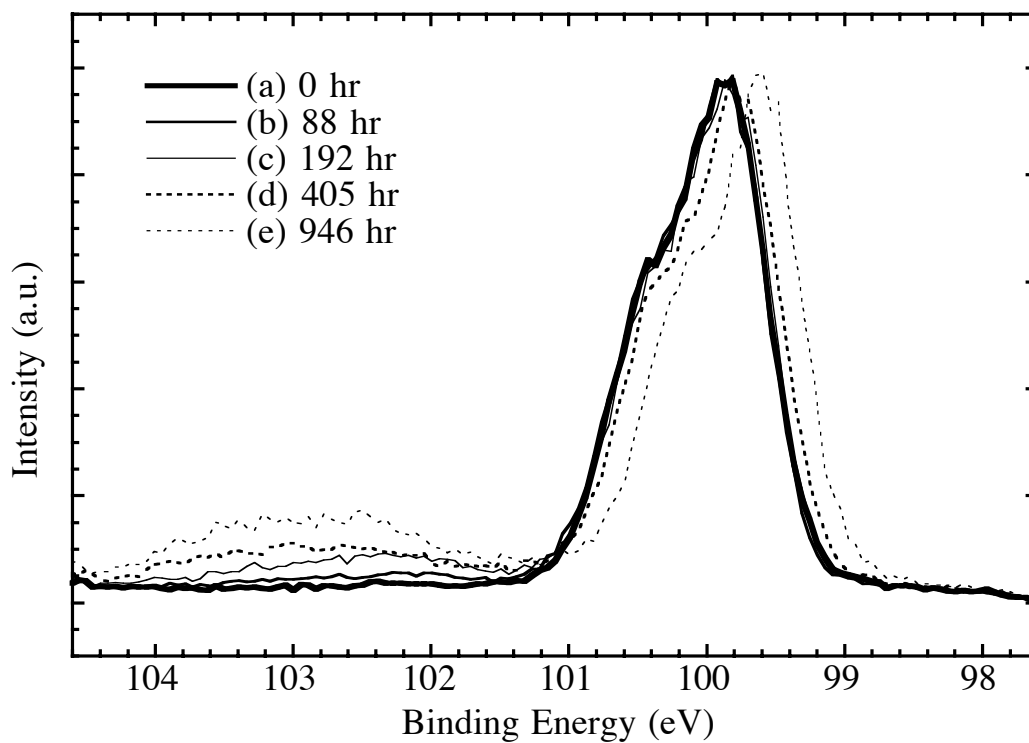


Figure 4.22

High-resolution XPS spectra of H-terminated Si focusing on the Si 2p region collected (a) before exposing the surface to the air, (b) after 88 hours, (c) after 192 hours, (d) after 405 hours, and (e) after 946 hours of air exposure, under low temperature/humidity condition. The samples were stored in a dark controlled environmental chamber with an air temperature of 21 °C and a relative humidity of 7% in between measurements. These spectra were normalized relative to the intensity of bulk Si 2p peak (99.2–101 eV binding energies).

Table 4.4

Time dependence of the silicon oxide growth for C5 olefin-terminated and C5 olefin-polyDCPD-terminated Si under both low and elevated temperature/humidity conditions, and for the H-terminate Si under low temperature/humidity condition.

Time Exposed to Air (hr)	Oxidized Si 2p /Bulk Si 2p	Calculated Oxide Layer Thickness ^a (nm)	Equivalent Monolayers SiO _x ^b
Si-C5 olefin in 21 °C/7% R.H.			
72	0.004	0.008	0.02
176	0.108	0.195	0.56
487	0.116	0.209	0.60
933	0.203	0.349	1.00
Si-C5 olefin in 40 °C/80–90% R.H.			
303	0.057	0.106	0.30
857	0.039	0.074	0.21
Si-C5 olefin-polyDCPD in 21 °C/7% R.H.			
70	0.064	0.120	0.34
174	0.386	0.607	1.73
384	0.471	0.713	2.04
931	0.799	1.063	3.04
Si-C5 olefin-polyDCPD in 40 °C/80–90% R.H.			
97	0.503	0.751	2.15
309	0.406	0.633	1.81
854	0.389	0.611	1.75
Si-H in 21 °C/7% R.H.			
88	0.037	0.070	0.20
192	0.072	0.134	0.38
405	0.121	0.219	0.62
946	0.226	0.383	1.10

^a Calculated using Equation 4.2, where the escape depth of the Si 2p electron through an oxide overlayer was taken to be 2.6 nm, $\theta = 35^\circ$, and the I_{Si}^0/I_{Ov}^0 in the Si 2p region was determined to be 1.3.

^b The thickness of a monolayer of SiO₂ was estimated to be 0.35 nm.

4. Discussions

4.1. Surface Modifications and Characterizations

Extended from the two-step chlorination/alkylation reaction developed previously in our laboratory, a reaction sequence was advanced for the modification of Si(111) surfaces with polymers. This method would appear to be general in that a wide range of monomers can be polymerized with **1**^{21,44,54,63} and could be used to form overlayers of controlled thicknesses on Si surfaces. When the first polymer layer is electrically insulating (as in the present case), this method should allow formation of metal-insulator-semiconductor structures or of capacitors of controlled thickness, whereas when the first polymer is metallic or semiconducting in nature (e.g., when cyclooctatetraenes, phenylenevinylenes, etc., are used as feedstocks⁶⁴), the process should provide a route to formation of semiconductor/metal or semiconductor heterojunction structures. Because the polymer was attached to the substrate through a covalent linkage, the polymer overlayer was robust and a relatively uniform growth was afforded as seen in SEM images.

Although XPS data were useful in providing evidences for each step of the surface modification process, there was a limitation that prevented us from obtaining a direct XPS confirmation for the binding of Ru catalysts to the olefin-terminated Si surfaces. The intensity of the Ru signal is expected to be very low when a relatively large amount of C can be detected on the surface. Assuming that reagent **1** has bound onto 50% of the total available groups in a monolayer of olefin on the Si surface implies a 1:41 Ru/C ratio for the atoms in the overlayer. With the atomic sensitivity factors of Ru 3d_{5/2} and C 1s being 1.55 and 0.205, respectively,⁶⁵ the area of the expected Ru 3d_{5/2} peak is calculated to be 18% of the C 1s signal. Because both the Ru 3d_{5/2} and Ru 3d_{3/2} peak

positions are within 5 eV of the C 1s peak, observation of such small Ru peaks in the presence of a large C 1s signal is not readily possible with our XPS instrument (VG Instruments M-probe Spectrometer, with a full width at half maximum of 1.50 ± 0.01 eV for the Au $4f_{7/2}$ peak in survey scan mode). Although the Ru $3p_{3/2}$ peak does not overlap with C 1s peak, the Ru $3p_{3/2}$ peak is about 1/3 as intense as the Ru $3d_{5/2}$ peak. Since the estimated relative peak area of the Ru $3p_{3/2}$ is only 6% of the C 1s peak area, it can not be resolved in the XP spectra of our polymer-terminated samples. Alternatively, the control experiments were used to establish the necessity of the presence of surface-bound Ru complexes for the formation of robust polymer overlayers. The presence of a polymer overlayer with a good coverage was also confirmed by the SEM results.

Both norbornene and DCPD were readily polymerized on Si surfaces using catalyst **1** as an initiator. Although bulk metathesis polymerization of COD using catalysts **1** and **2** and COT using catalyst **2** has been reported previously,^{64,66} surface-initiated ROMP of either COD or COT on Si(111) was not successful. When a Si surface was first coated with catalyst **1** by adding a few drops of 25 mM catalyst solution and the solvent was allowed to evaporate, a polymer film was observed following addition of COD to the catalyst-coated Si. The result suggested that while the surface-bound Ru catalyst was able to ROMP the highly strained norbornene; the concentration of surface-bound catalyst may not be high enough to permit detectable surface-initiated ROMP of less-strained COD and COT. The binding of a Ru complex to an olefin linker requires the complex to line up with the double bond of the linker in a certain way, and this can be quite difficult when the linker is fixed on the Si surface. The large dimensions of Ru molecules also post a geometric limitation (see Figure 4.23) which does not allow all olefin linkers on the substrate to bind with Ru; therefore, the low concentration of the surface-bound catalyst is suspected to impede the successful ROMP of less-strained ring monomers.

Another problem encountered during the Si surface modification process was the possible introduction of silicon oxide. The surface modification process involved was very sensitive to any oxygen source including methanol vapor that might be present in the $N_2(g)$ -purged glove box. When the surface modification took place without first eliminating as much methanol vapor as possible, and when septa-capped test tubes were used instead of screw-capped, the success rate for producing oxide-free modified surfaces was very low. During the overnight heated Grignard reaction, the methanol vapor can be drawn into the reaction vessels and can provide the Si with oxygen needed for oxidation. By placing a wide-mouth bottle containing fresh P_2O_5 powders in the glove box before and during the reaction, the P_2O_5 could absorb methanol vapor and reduced the amount of volatile oxygen source. The reaction tubes were also capped tightly to ensure minimal exposure of the reaction contents to the glove box atmosphere.

Other factors that might affect the success rate of surface modification include the freshness of reagents and the possibility of the contamination of rinsing solvents. While the monomer solutions can be stored in aluminum foil-wrapped Schlenk tubes inside the glove box, it is best to use freshly made monomer solutions to assure that the correct monomer concentration was used. There is always a possibility for monomers to polymerize in the Schlenk tube if the solution was contaminated by any catalyst molecule, and this could lead to a lower than expected monomer concentration for polymerization on the substrate. The Grignard reagents purchased from Aldrich should only be used within one month after opening the bottle in the glove box. It is also best to keep the Sure/Seal caps on for all solvents and reagents, and use only syringes to dispense all liquids.

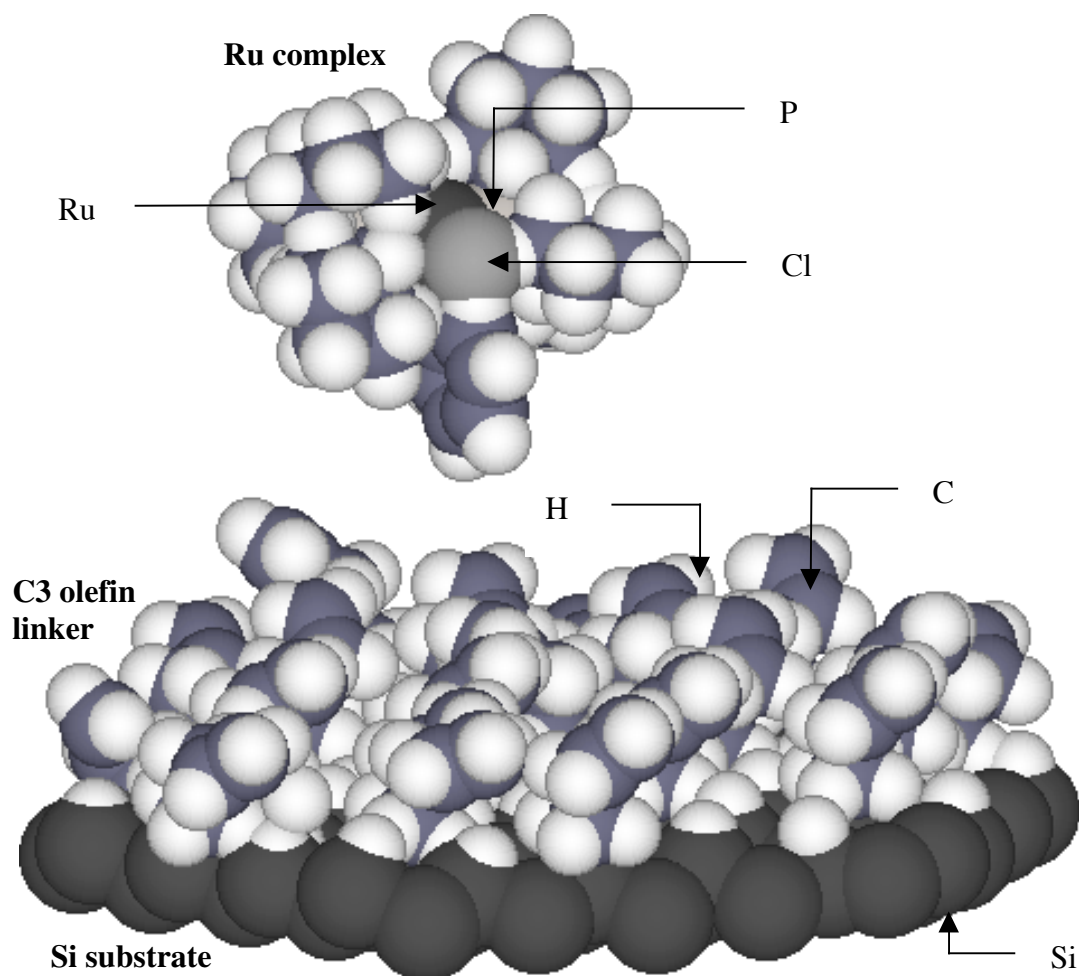


Figure 4.23

A space-filling model showing the relative sizes of the Ru catalyst and the Si surface atoms. The Si surface is covered with C3 olefin linkers. Since the cross section of a Ru complex is much larger than that of an olefin linker, the number of surface-bound Ru molecules is expected to be less than 50% of the number of linkers. The Ru addition requires a cross metathesis reaction between the Ru=C double bond and the terminal C=C double bond of the olefin linker.

4.2. Surface Recombination Velocity and Oxidation

The transient photoconductivity decay behaviors of modified Si surfaces were studied to further investigate the effects of surface modification on the electrical properties of Si. The results indicated the lack of silicon oxide formation during the surface-initiated ROMP of both norbornene and DCPD, and covalently attached polymer overlayers were grown on the Si surfaces. The initial photoconductivity decay measurements of C3 olefin-terminated, C3 olefin-polybornene-terminated, and C3 olefin-polyDCPD-terminated Si in an N₂(g) ambient showed that the surface modification procedure did not greatly affect the desirable electrical properties of Si, and all three types of surfaces exhibited low defect density following the reactions. However, the charge-carrier recombination lifetimes decreased quickly upon exposure to an air ambient, suggesting that the attached overlayers were ineffective in preventing the surface degradation of Si in air. When the time dependence of mean carrier lifetimes of these three surfaces were compared, the rates of decreasing lifetime were slower for both polymer-terminated surfaces, despite having shorter initial lifetimes than that of olefin-terminated Si.

When longer terminal olefin linkers, specifically C5 and C6 olefins, were used, the mean carrier lifetimes did not drop upon air exposure. In fact, C5 olefin-terminated surface was found to have an initial lifetime $>350 \mu\text{s}$, and was capable of preserving the long lifetime for at least 300 hours in air. Presumably the C5 and C6 olefin chains were more flexible while fixed onto the Si surfaces, the slight tilt of these chains could possibly cover some potential oxidation sites and decrease the chances of defect formation. Subsequent growth of polymer overlayers on top of the C5 olefin resulted in slightly shorter initial lifetimes, but both C5 olefin-polybornene- and C5 olefin-polyDCPD-terminated Si were capable of keeping the mean carrier lifetimes at

200–300 μs for about one month. The surface recombination velocity can be related to the surface defect density using the equation:^{12,57}

$$2S = N_t v_{th} \sigma \quad (3.3)$$

where N_t is the number of recombination centers per square centimeter, v_{th} is the carrier thermal velocity (taken to be $\approx 10^7 \text{ cm s}^{-1}$), and σ is the carrier-capture cross section. Assuming the σ is 10^{-15} cm^2 , these polymer-terminated Si surfaces would have surface defect density of $(0.98\text{--}1.5) \times 10^{10} \text{ cm}^{-2}$. This is equivalent to having a low defect density of less than one active electrical defect site for every $\approx 68,000$ surface atoms. This surface modification sequence using C5 olefin as a linker could therefore prove useful in providing means to functionalize Si without jeopardizing the electrical properties necessary for device applications.

While further XPS analysis of C5 olefin- and C5 olefin-polyDCPD-terminated surfaces revealed silicon oxide formation in an air ambient, the persisting slow surface recombination velocities indicated that the polymer overlayers were still effective in preventing electrical degradation of Si when oxidized. The oxide layer thickness was calculated with an assumption that ejected electrons from both bulk Si and Si oxide were attenuated by the polymer overlayer of a uniform density and thickness. However, if the oxide only grew from Si atoms that were not modified due to geometric limitation of the olefin linker, it is possible that the region of polymer overlayer above the oxide was less dense than the region above a grafting point. In this case, a larger portion of total electrons ejected from Si oxide would escape through the polymer overlayer and being collected by the analyzer compared to the number of escaped electrons originated from the bulk Si. The result would then be translated into a larger oxidized/bulk Si 2p peak ratio and a thicker calculated oxide film. The unusually large oxidized Si oxide peaks observed in the XP spectra of the polyDCPD-terminated surface may be the consequence

of this density variation, and the reported Si oxide thicknesses for these samples may not represent the true values.

Figure 4.24 displays the Si 2p high-resolution XP spectra of oxidized H-terminated, C5 olefin-terminated, and C5 olefin-polyDCPD-terminated Si surfaces after ~930 hours of air exposure under low temperature/humidity condition. A comparison of the oxidized Si 2p peak positions of these samples was made to elucidate the differences in surface oxides that gave rise to very different S . When spectra were shifted to line up bulk Si 2p peaks of these three surfaces, the Si oxide peaks of both C5 olefin-terminated and polyDCPD-terminated surfaces appeared at a slightly higher binding energy compared to that of the air-oxidized H-terminated surface. This finding suggests that a different kind of Si oxide was formed when C5 olefin-terminated and C5 olefin-polymer-modified Si were exposed to air, and this oxide formation did not create additional surface defects that could cause the S to rise. The oxide thickness was very similar between H-terminated and C5 olefin-terminated Si oxidized under the low temperature/humidity condition, but the carrier lifetime of the H-terminated Si was substantially shorter, recorded at as low as $6 \mu\text{s}$ after 900 hours of air exposure. The ability for C5 olefin-polymer-terminated Si to persist low surface defect density despite the formation of Si oxide when stored in air under both low and elevated temperature/humidity conditions proved the excellence and usefulness of this general surface modification method. This reaction sequence can provide a simple route to grow robust and uniform overlayers of polymers and block copolymers with different functionalities on Si surfaces, especially for novel applications in electrical devices requiring low surface recombination velocity.

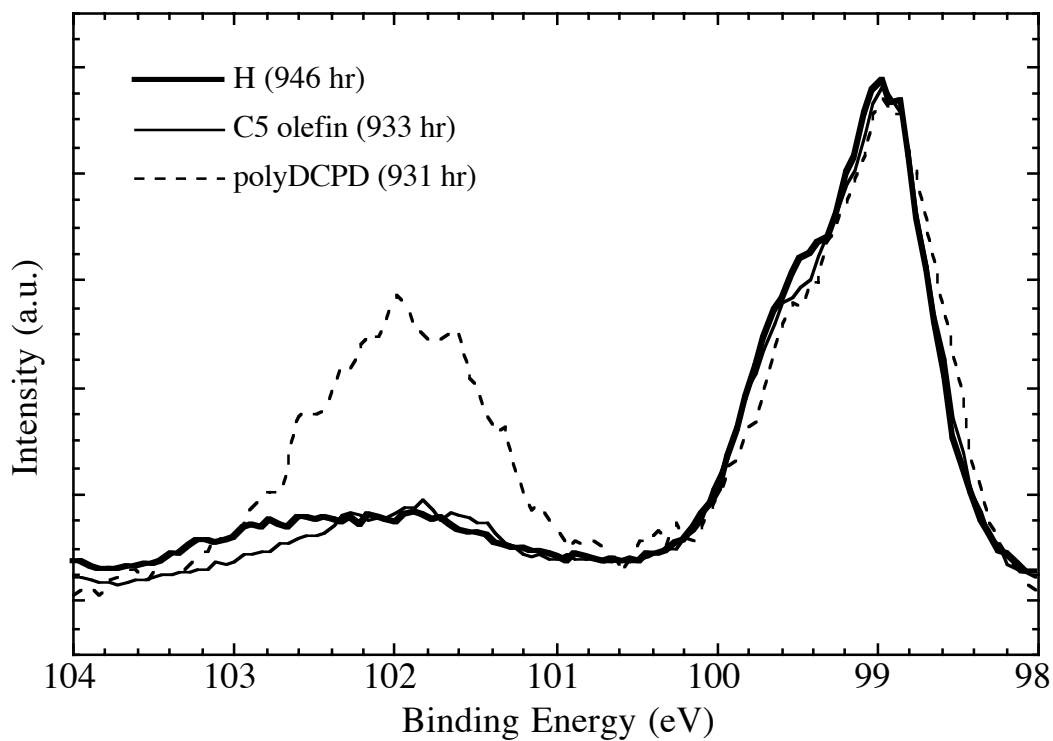


Figure 4.24

The Si 2p high-resolution XP spectra of H-terminated (———), C5 olefin-terminated (———), and C5 olefin-polyDCPD-terminated (- - - - -) surfaces. The spectra were normalized relative to the intensity of bulk Si 2p peak. The silicon oxide peak positions of both polymer-terminated surfaces shifted to slightly lower binding energy, indicating a different kind of silicon oxide was formed.

5. Summary

The growth of robust polymer films that are covalently attached to Si surfaces via a Si-C linkage was demonstrated. Uniform layers of different polymers were formed using a general method combining chlorination/Grignard reaction with ring-opening metathesis polymerization (ROMP). The surfaces of these modified Si were characterized by XPS, SEM, ellipsometry, and/or profilometry. Varying the concentration of monomer can control the thickness of the polymer overlayer, so that polymer thicknesses between 0.9 and 5500 nm can be achieved. The charge-carrier dynamics at olefin- and polymer-terminated Si/air interfaces was investigated using transient photoconductivity decay method. The C5 olefin was determined to be the optimal linker that is capable of preserving the electrical properties of the Si(111) surface when exposed to air. Time-dependent photoconductivity measurements further confirmed the ability for both polynorbornene-terminated and polyDCPD-terminated Si to maintain low surface recombination velocities in air for a period of one month, under both low and elevated temperature/humidity conditions. Instead of acting as a physical barrier against oxidation, the polymer overlayer allows the formation of non-deleterious Si oxide that does not introduce defect site on the surface. This “graft from” method is proven to be a general and simple way to modify Si surfaces with cyclic and derivatized cyclic polymers for future electronic device applications.

6. Acknowledgments

I thank Oren A. Scherman for the collaboration and for the synthesis of Grignard reagents. This work was supported by the National Science Foundation, CHE-9974562 (N.S.L.), and by the Air Force Office of Scientific Research, Grant F49620-96-0035 (R.H.G.).

7. References

- (1) Bansal, A.; Lewis, N. S. *J. Phys. Chem. B* **1998**, *102*, 4058.
- (2) Sailor, M. J.; Klavetter, F. L.; Grubbs, R. H.; Lewis, N. S. *Nature* **1990**, *346*, 155.
- (3) Huck, W. T. S.; Yan, L.; Stroock, A.; Haag, R.; Whitesides, G. M. *Langmuir* **1999**, *15*, 6862.
- (4) Clark, S. L.; Montague, M.; Hammond, P. T. *Supramol. Sci.* **1997**, *4*, 141.
- (5) Whidden, T. K.; Ferry, D. K.; Kozicki, M. N.; Kim, E.; Kumar, A.; Wilbur, J.; Whitesides, G. M. *Nanotechnology* **1996**, *7*, 447.
- (6) Sailor, M. J.; Ginsburg, E. J.; Gorman, C. B.; Kumar, A.; Grubbs, R. H.; Lewis, N. S. *Science* **1990**, *249*, 1146.
- (7) Bansal, A.; Lewis, N. S. *J. Phys. Chem. B* **1998**, *102*, 1067.
- (8) Royea, W. J.; Juang, A.; Lewis, N. S. *Appl. Phys. Lett.* **2000**, *77*, 1988.
- (9) Sze, S. M. *The Physics of Semiconductor Devices*; 2nd ed.; Wiley: New York, 1981.
- (10) Royea, W. J.; Michalak, D. J.; Lewis, N. S. *Appl. Phys. Lett.* **2000**, *77*, 2566.
- (11) Eades, W. D.; Swanson, R. M. *J. Appl. Phys.* **1985**, *58*, 4267.
- (12) Yablonovitch, E.; Gmitter, T. J. *Solid State Elec.* **1992**, *35*, 261.
- (13) Aberle, A. G.; Glunz, S.; Warta, W. *J. Appl. Phys.* **1992**, *71*, 4422.
- (14) Ulman, A. *An Introduction to Ultrathin Organic Films*; Academic Press: Boston, 1991.
- (15) Hadziioannou, G.; Patel, S.; Granick, S.; Tirrell, M. *J. Am. Chem. Soc.* **1986**, *108*, 2869.
- (16) Belder, G. F.; tenBrinke, G.; Hadziioannou, G. *Langmuir* **1997**, *13*, 4102.
- (17) Dan, N.; Tirrell, M. *Macromolecules* **1993**, *26*, 6467.
- (18) Lenk, T. J.; Hallmark, V. M.; Rabolt, J. F.; Haussling, L.; Ringsdorf, H. *Macromolecules* **1993**, *26*, 1230.
- (19) Jordan, R.; Graf, K.; Riegler, H.; Unger, K. K. *Chem. Commun.* **1996**, 1025.
- (20) Ebata, K.; Furukawa, K.; Matsumoto, N. *J. Am. Chem. Soc.* **1998**, *120*, 7367.
- (21) Kim, N. Y.; Jeon, N. L.; Choi, I. S.; Takami, S.; Harada, Y.; Finnie, K. R.; Girolami, G. S.; Nuzzo, R. G.; Whitesides, G. M.; Laibinis, P. E. *Macromolecules* **2000**, *33*, 2793.
- (22) Jordan, R.; Ulman, A. *J. Am. Chem. Soc.* **1998**, *120*, 243.
- (23) Jordan, R.; Ulman, A.; Kang, J. F.; Rafailovich, M. H.; Sokolov, J. *J. Am. Chem. Soc.* **1999**, *121*, 1016.
- (24) Prucker, O.; Ruhe, J. *Macromolecules* **1998**, *31*, 602.

- (25) Zhao, B.; Brittain, W. J. *Macromolecules* **2000**, *33*, 8813.
- (26) Ingall, M. D. K.; Joray, S. J.; Duffy, D. J.; Long, D. P.; Bianconi, P. A. *J. Am. Chem. Soc.* **2000**, *122*, 7845.
- (27) Husseman, M.; Malmstrom, E. E.; McNamara, M.; Mate, M.; Mecerreyes, D.; Benoit, D. G.; Hedrick, J. L.; Mansky, P.; Huang, E.; Russell, T. P.; Hawker, C. J. *Macromolecules* **1999**, *32*, 1424.
- (28) Boukherroub, R.; Wayner, D. D. M. *J. Am. Chem. Soc.* **1999**, *121*, 11513.
- (29) Sieval, A. B.; Vleeming, V.; Zuilhof, H.; Sudholter, E. J. R. *Langmuir* **1999**, *15*, 8288.
- (30) Boukherroub, R.; Morin, S.; Bensebaa, F.; Wayner, D. D. M. *Langmuir* **1999**, *15*, 3831.
- (31) Sieval, A. B.; Demirel, A. L.; Nissink, J. W. M.; Linford, M. R.; van der Maas, J. H.; de Jeu, W. H.; Zuilhof, H.; Sudholter, E. J. R. *Langmuir* **1998**, *14*, 1759.
- (32) Linford, M. R.; Chidsey, C. E. D. *J. Am. Chem. Soc.* **1993**, *115*, 12631.
- (33) Linford, M. R.; Fenter, P.; Eisenberger, P. M.; Chidsey, C. E. D. *J. Am. Chem. Soc.* **1995**, *117*, 3145.
- (34) Zazzera, L. A.; Evans, J. F.; Deruelle, M.; Tirrell, M.; Kessel, C. R.; Mckeown, P. *J. Electrochem. Soc.* **1997**, *144*, 2184.
- (35) Feng, W. J.; Miller, B. *Langmuir* **1999**, *15*, 3152.
- (36) Effenberger, F.; Gotz, G.; Bidlingmaier, B.; Wezstein, M. *Angew. Chem.-Int. Edit.* **1998**, *37*, 2462.
- (37) Allongue, P.; de Villeneuve, C. H.; Pinson, J.; Ozanam, F.; Chazalviel, J. N.; Wallart, X. *Electrochim. Acta* **1998**, *43*, 2791.
- (38) He, J.; Patitsas, S. N.; Preston, K. F.; Wolkow, R. A.; Wayner, D. D. M. *Chem. Phys. Lett.* **1998**, *286*, 508.
- (39) deVilleneuve, C. H.; Pinson, J.; Bernard, M. C.; Allongue, P. *J. Phys. Chem. B* **1997**, *101*, 2415.
- (40) Wagner, P.; Nock, S.; Spudich, J. A.; Volkmuth, W. D.; Chu, S.; Cicero, R. L.; Wade, C. P.; Linford, M. R.; Chidsey, C. E. D. *J. Struct. Biol.* **1997**, *119*, 189.
- (41) Hamers, R. J.; Coulter, S. K.; Ellison, M. D.; Hovis, J. S.; Padowitz, D. F.; Schwartz, M. P.; Greenlief, C. M.; Russell, J. N. *Accounts Chem. Res.* **2000**, *33*, 617.
- (42) Schwartz, M. P.; Ellison, M. D.; Coulter, S. K.; Hovis, J. S.; Hamers, R. J. *J. Am. Chem. Soc.* **2000**, *122*, 8529.
- (43) Bansal, A.; Li, X.; Lauermaun, I.; Lewis, N. S.; Yi, S. I.; Weinberg, W. H. *J. Am. Chem. Soc.* **1996**, *118*, 7225.

- (44) Weck, M.; Jackiw, J. J.; Rossi, R. R.; Weiss, P. S.; Grubbs, R. H. *J. Am. Chem. Soc.* **1999**, *121*, 4088.
- (45) Scholl, M.; Ding, S.; Lee, C. W.; Grubbs, R. H. *Org. Lett.* **1999**, *1*, 953.
- (46) Higashi, G. S.; Chabal, Y. J.; Trucks, G. W.; Raghavachari, K. *Appl. Phys. Lett.* **1990**, *56*, 656.
- (47) Hassler, K.; Koll, W. *J. Organomet. Chem.* **1995**, *487*, 223.
- (48) Wyman, D. P.; Wang, J. Y. C.; Freeman, W. R. *J. Org. Chem.* **1963**, *28*, 3173.
- (49) Stinespring, C. D.; Wormhoudt, J. C. *J. Appl. Phys.* **1989**, *65*, 1733.
- (50) Cheng, K. L. *Japan. J. Appl. Phys.* **1995**, *34*, 5527.
- (51) Tufts, B. J.; Kumar, A.; Bansal, A.; Lewis, N. S. *J. Phys. Chem.* **1992**, *96*, 4581.
- (52) Mende, G.; Finster, J.; Flamm, D.; Schulze, D. *Surf. Sci.* **1983**, *128*, 169.
- (53) Schwab, P.; Grubbs, R. H.; Ziller, J. W. *J. Am. Chem. Soc.* **1996**, *118*, 100.
- (54) Amir-Ebrahimi, V.; Corry, D. A.; Hamilton, J. G.; Thompson, J. M.; Rooney, J. J. *Macromolecules* **2000**, *33*, 717.
- (55) Kunst, M.; Sanders, A. *Semicond. Sci. Technol.* **1992**, *7*, 51.
- (56) Yablonovitch, E.; Swanson, R. M.; Eades, W. E.; Weinberger, B. R. *Appl. Phys. Lett.* **1986**, *48*, 245.
- (57) Yablonovitch, E.; Allara, D. L.; Chang, C. C.; Gmitter, T.; Bright, T. B. *Phys. Rev. Lett.* **1986**, *57*, 249.
- (58) Bansal, A.; Li, X.; Yi, S. I.; Weinberg, W. H.; Lewis, N. S. *J. Phys. Chem. B* **2001**, *105*, 10266.
- (59) Briggs, D.; Seah, M. P. *Practical Surface Analysis: Auger and X-Ray Photoelectron Spectroscopy*; 2nd ed.; Wiley: New York, 1990; Vol. 1.
- (60) Pomykal, K. E.; Fajardo, A. M.; Lewis, N. S. *J. Phys. Chem.* **1995**, *99*, 8302.
- (61) Hochella, M. F., Jr.; Carim, A. H. *Surf. Sci.* **1988**, *197*, L260.
- (62) Haber, J. A.; Lewis, N. S. *J. Phys. Chem. B* **2002**, *106*, 3639.
- (63) Maughon, B. R.; Morita, T.; Bielawski, C. W.; Grubbs, R. H. *Macromolecules* **2000**, *33*, 1929.
- (64) Scherman, O. A.; Grubbs, R. H. *Synth. Metals* **2001**, *124*, 431.
- (65) Wagner, C. D.; Riggs, W. M.; Davis, L. E.; Moulder, J. F. *Handbook of X-Ray Photoelectron Spectroscopy*; Perkin-Elmer Corporation: Eden Prairie, MN, 1979.
- (66) Bielawski, C. W.; Scherman, O. A.; Grubbs, R. H. *Polymer* **2001**, *42*, 4939.